An Enhanced Deadbeat Predictive Current Control of SPMSM with Linear Disturbance Observer

Journal:	*Journal of Emerging and Selected Topics in Power Electronics*
Manuscript ID	JESTPE-2021-12-1420.R1
Manuscript Type:	Regular Paper
Date Submitted by the Author:	09-Feb-2022
Complete List of Authors:	Yuan, Xin; Nanyang Technological University, School of Electrical and Electronic Engineering XIE, Shuangchun; Nanyang Technological University, School of Electrical and Electronical Engineering Chen, Jiahao; Nanyang Technological University, School of EEE; Zhejiang University, College of Electrical Engineering Zhang, Shuo; Beijing Institute of Technology, Mechanical Engineering Zhang, Chengning; School of Mechanical Engineering, Beijing Institute of Technology, Department of vehicle Engineering Lee, Christopher H. T. ; Nanyang Technological University, School of Electrical & Electronic Engineering
Keywords:	Permanent magnet synchronous motor(s) (PMSM), Dead-beat control (DBC), Disturbance observer (DOB)
Subject Category:	Renewable Energy

An Enhanced Deadbeat Predictive Current Control of SPMSM with Linear Disturbance Observer

Xin Yuan, *Member IEEE*, Shuangchun Xie, *Student Member IEEE*, Jiahao Chen, *Member IEEE*, Shuo Zhang, *Member IEEE*, Chengning Zhang and Christopher H. T. Lee, *Senior Member IEEE*

***Abstract*—Deadbeat predictive current control (DPCC) with linear disturbance observer (LDO) in surface-mounted permanent magnet synchronous machine (SPMSM) has been widely applied in many applications owing to better dynamic response performance and easy implementation. However, the evaluated lumped disturbances caused by current measurement noises, inverter nonlinearity, abrupt reference current and initial inductance parameter mismatch can restrain the high performance development. In order to handle this issue, an enhanced DPCC with LDO is proposed in this paper, where a modified DPCC with LDO model and non-invasive inductance and inverter disturbance observer are developed. In this case, the initial inductance parameter mismatch and high frequency disturbances effect on the DPCC with LDO is reduced while the current measurement noises suppression is enhanced by the proposed LDO. The theoretical analysis has shown that the proposed DPCC with LDO has better performance than the conventional DPCC with LDO. Also, the superiority of the proposed DPCC with LDO has been validated by an SPMSM drive test rig.**

***Index Terms*—Deadbeat predictive current control (DPCC), Surface-mounted permanent magnet synchronous machine (SPMSM), Linear disturbance observer (LDO), Inverter nonlinearity.**

NOMENCLATURE

$U_d^{'}, U_q^{'}$	dq-axis inverter nonlinearity distorted voltage
$U_\alpha^{'}, U_\beta^{'}$	$\alpha\beta$-axis inverter nonlinearity distorted voltage
U_d^{ref}, U_q^{ref}	dq-axis inverter output reference voltage
i_d, i_q	dq-axis stator actual current
i_d^{ref}, i_q^{ref}	dq-axis stator reference current
$\hat{i}_d, \hat{i}_q$	dq-axis predicted stator current of LDO
ω_e, T_s	Electrical angular speed and control period
L_s, R_s	Actual stator inductance and resistance
ψ_m, θ_e	Actual rotor flux linkage and electrical angle
T_e, T_l	Electromagnetic torque and load torque
L_{s0}	Nominal stator inductance in controller
w_n	Undamped natural frequency of LDO

I. Introduction

DUE to the merits of high efficiency and high power density, permanent magnet synchronous machine (PMSM) has been widely applying in industrial applications [1]. Recently, predictive control has been attracting increasing attention due to high dynamic response and low calculation burden [2]. Generally, predictive control can be divided into two parts, namely, predictive control with pulse width modulation (PWM) technique and predictive control without PWM technique. In the predictive control without PWM, a typical method is model predictive current control (MPCC) where it is able to predict future optimum finite voltage vectors generated by inverters based on cost function minimization. Deadbeat predictive current control (DPCC) belongs to the predictive control with PWM, and it can generate a desired reference voltage vector by employing PWM. Compared with MPCC, DPCC owns the merits of fixed switching frequency and low calculation [3], [4]. Nevertheless, in contrast to proportional-integral (PI) control [5] that inherently possesses certain abilities to suppress disturbances, a main barrier for the DPCC development is the lack of disturbances suppression [6]. Normally, main disturbances in current loop system can occur as follows: (i) PMSM parameter mismatch disturbance, i.e., PMSM parameters vary under different operations. E.g., the value of stator inductance decreases as the stator current rises, and the values of stator resistance increases and rotor flux linkage reduces as the environment temperature increases [7]. (ii) Inverter parameter disturbance, i.e, the magnitudes of deadtime voltage and distorted voltage caused by inverter nonlinearity vary with the different values of dc bus voltage [8]. The disturbance suppression approaches are categorized into invasive and non-invasive identification approaches in this paper, as summarized in Fig.1.

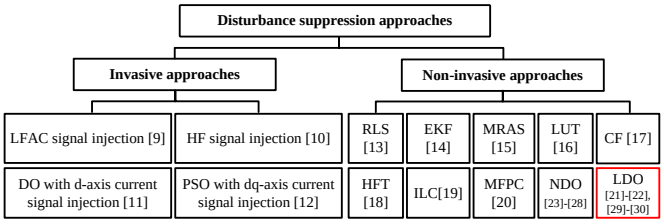

Fig. 1. Diagram of disturbance suppression approaches.

Regarding to invasive identification approaches, an identification of the machine magnetic model using low frequency-AC (LFAC) signal injection is proposed [9], where the machine inductance parameter can be identified with or without rotor locking. Wang et al. proposed an high frequency (HF) equivalent impedance PMSM model, in which HF signal injection can be carried out on dq-axis to obtain the PMSM multi-parameters [10]. An improved DPCC is developed [11], where a disturbance observer (DO) with d-axis current signal injection is developed to improve the DPCC dynamic response performance. Furthermore, an improved particle swarm optimization (PSO) with dq-axis current injection is proposed

to construct another set of motor states for machine multi-parameters identification [12]. However, the invasive methods can induce unnecessary voltage or current harmonics and hence negatively affect the system control performance.

Based on machine voltage equations, effective non-invasive disturbance suppression approaches have been developed. The three popular parameter identifications below have been developed. Recursive least-squares (RLS) algorithm is able to identify machine parameters based on the minimum least square error principle [13]. Extended Kalman filter (EKF) is developed to enhance the accuracy of model parameter identification [14] but the calculation is relatively large contrasted with RLS. A model reference adaptive system (MRAS) estimator is developed to estimate parts of machine parameters by fixing the rest parameters to their nominal values [15]. However, the machine voltage equation rank deficiency occurs under the identification of multiple parameters and hence the estimation accuracy will be deteriorated. Two typical offline parameter identifications can be considered as an alternative, i.e., look-up-table (LUT) [16] and curve fitting (CF) [17]. However, the obtained parameters from offline LUT or CF coefficients may suffer from disturbances under uncertainty operations. In addition, a harmonic filtering technology (HFT) is employed to filter useful sixth order harmonic voltages where the inverter disturbance parameters can be acquired [18], but the limitation is that the disturbances caused by higher order harmonics are neglected.

In order to obtain lumped disturbances instead of single or multiple parameters identification, model-based observers have been getting more attention. With regard to suppressing periodical disturbances, iterative learning control (ILC) can be effectively employed based on the ILC law principle [19]. To acquire the total disturbances caused by resistance, inductance and rotor flux linkage mismatch, a model-free predictive controller (MFPC) based on current variation update mechanism is proposed [20], but this method can only work through finite output voltage vectors and hence is more suitable in MPCC. Regarding to the non-periodical disturbances suppression, DO has been designed [21]–[23]. The basic point of the observer is to reconstruct a controlled state by designing a suitable deviation between the actual state and predicted state matrix. Generally, DO can be classified into nonlinear DO (NDO) and linear DO (LDO) in control theory. In contrast to LDO, NDO is more complex and the designed coefficients of NDO are relatively difficult to be determined, but the faster convergence speed can be achieved depending on the nonlinear property. SMDO is one of NDOs and can force system track a setting trajectory at high frequency and small amplitude move [24]. Combining SMDO with the super-twisting sliding mode technique, a composite super-twisting SMOD is proposed to improve the performance of the closed-loop SPMSM speed system, in which the gain of the composite sliding mode controller can be significantly reduced [25]. In order to estimate disturbances more quickly and precisely, a nonlinear high-gain disturbance observer is proposed [26]. In addition, a high order disturbance observer is developed to cope with ramp and general order disturbances and the noise effect on the NDO is reduced [27]. An improved DPCC with SMDO is proposed to evaluate the lumped disturbances caused by current loop parameter mismatch [28]. Because of the simple calculation, LDO is widely applied in various industrial applications. Kim et al. utilized LDO to compensate the deadtime voltage disturbance caused by inverter nonlinearity [29]. An improved DPCC with LDO is proposed to overcome the disturbance caused by PMSM parameter mismatch [30].

Due to the merits, i.e., fast dynamic response, adjustable disturbance rejection and easy implementation, DPCC with LDO has been widely utilized in surface-mounted PMSM (SPMSM) drives. However, the LDO bandwidth is a trade-off between current measurement noises and disturbance rejection. High frequency disturbances cannot be completely suppressed, restraining the high performance current controller development at some extent. Motivated by this argument, an enhanced DPCC with LDO is proposed and the contribution of this work can be listed as follows.

(i) This paper has extended far beyond [28]–[30]. First, the limitation of the conventional DPCC with LDO is analyzed in detail. It is unrealistic to estimate high frequency disturbances by employing the LDO due to the limited LDO bandwidth. It will be clarified that the evaluated disturbances caused by current measurement noises, inverter nonlinearity, abrupt reference current and initial inductance parameter mismatch can restrain the high performance of the conventional DPCC with LDO.

(ii) With regard to further enhancing DPCC with LDO and suppressing the above limitations effect on DPCC with LDO, an enhanced DPCC with LDO is proposed. In the proposed structure, unlike the DPCC with LDO [30], the modified DPCC with LDO model is developed and the proposed LDO can exhibit better current measurement noises suppression. The disturbances caused by inverter nonlinearity and dq-axis coupling inductance voltage are not considered in lumped disturbances of the LDO and hence the high frequency disturbances caused by inverter nonlinearity and abrupt q-axis reference current effect on the current loop system will be suppressed. Furthermore, in order to eliminate the initial inductance parameter mismatch effect on the DPCC with LDO, different from the invasive d-axis current injection approach [11], a non-invasive inductance and inverter disturbance observer without employing any inverter and SPMSM parameters is developed, where the proposed observer can acquire the actual inductance parameter and inverter disturbance based on current and position sensors.

The rest of this paper is structured as follows. Section II introduces the conventional DPCC with LDO. The limitation of the conventional DPCC with LDO is illustrated in Section III. The detailed procedure of the proposed DPCC with LDO is presented in Section IV. Experiment of the three different DPCC methods i.e., the conventional DPCC, DPCC with LDO [30] and proposed DPCC with LDO are carried out in Section V. Finally, the conclusions are derived in Section VI.

II. Conventional DPCC Using LDO

To simplify the SPMSM mathematical model, the following factors need to be neglected: magnetic saturation and cross-

saturation. The SPMSM voltage equations considering inverter nonlinearity are presented as follows:

$$\begin{cases} U_d^{ref} = L_s\dfrac{di_d}{dt} + R_s i_d - \omega_e L_s i_q + U_d^{'} \\ U_q^{ref} = L_s\dfrac{di_q}{dt} + R_s i_q + \omega_e L_s i_d + \omega_e \psi_m + U_q^{'} \end{cases} \tag{1}$$

where $\frac{di_d}{dt}, \frac{di_q}{dt}$ mean the differential of the dq-axis stator currents, respectively.

A. Conventional DPCC

In practical digital systems, considering the one-step delay issue, the first order forward Euler discretization is employed to obtain the (k+1)th instant stator current, as shown as:

$$\mathbf{i_{dq}(k+1)} = \mathbf{A i_{dq}(k)} + \mathbf{B}[\mathbf{U_{dq}^{ref}(k)} - \mathbf{U_{dq}^{'}(k)}] + \mathbf{C} \tag{2}$$

where $\mathbf{A} = \begin{bmatrix} 1-\frac{T_s R_s}{L_s} & T_s\omega_e(k) \\ -T_s\omega_e(k) & 1-\frac{T_s R_s}{L_s} \end{bmatrix}$, $\mathbf{B} = \begin{bmatrix} \frac{T_s}{L_s} & 0 \\ 0 & \frac{T_s}{L_s} \end{bmatrix}$, $\mathbf{C} = \begin{bmatrix} 0 \\ -\frac{T_s\psi_m}{L_s}\omega_e(k) \end{bmatrix}$, $\mathbf{i_{dq}} = \begin{bmatrix} i_d \\ i_q \end{bmatrix}$, $\mathbf{U_{dq}^{ref}} = \begin{bmatrix} U_d^{ref} \\ U_q^{ref} \end{bmatrix}$, $\mathbf{U_{dq}^{'}} = \begin{bmatrix} U_d^{'} \\ U_q^{'} \end{bmatrix}$. It should be noted that the electrical angular at adjacent control period can be assumed as the same since the SPMSM electrical time constant is relativity shorter than the mechanical time constant. Based on the DPCC principle, the (k+1)th instant reference voltage can be presented as:

$$\mathbf{U_{dq}^{ref}(k+1)} = \mathbf{D i_{dq}^{ref}(k)} + \mathbf{E i_{dq}(k+1)} + \mathbf{F} \tag{3}$$

where $\mathbf{D} = \begin{bmatrix} \frac{L_s}{T_s} & 0 \\ 0 & \frac{L_s}{T_s} \end{bmatrix}$, $\mathbf{E} = \begin{bmatrix} R_s - \frac{L_s}{T_s} & -L_s\omega_e(k) \\ L_s\omega_e(k) & R_s - \frac{L_s}{T_s} \end{bmatrix}$, $\mathbf{F} = \begin{bmatrix} 0 \\ \omega_e(k)\psi_m \end{bmatrix} + \mathbf{U_{dq}^{'}(k+1)}$, $\mathbf{i_{dq}^{ref}} = \begin{bmatrix} i_d^{ref} \\ i_q^{ref} \end{bmatrix}$. However, it is well known that disturbances caused by SPMSM model parameter mismatch and inverter nonlinearity can deteriorate the conventional DPCC.

B. DPCC with LDO

In order to suppress the disturbance effect on DPCC performance, the DPCC with LDO is proposed [30], presented as follows.

1) Taking total disturbances $\widehat{\mathbf{D_{dq1}}}$ and stator current $\mathbf{i_{dq}}$ as state variables, the DPCC with LDO can be expressed as follows:

$$\begin{cases} \mathbf{e_{rr}(k)} = \widehat{\mathbf{i_{dq}}}\mathbf{(k)} - \mathbf{i_{dq}(k)} \\ \widehat{\mathbf{i_{dq}}}\mathbf{(k+1)} = \widehat{\mathbf{i_{dq}}}\mathbf{(k)} + \dfrac{T_s}{L_{s0}}\mathbf{U_{dq}^{ref}(k)} + \widehat{\mathbf{D_{dq1}}}\mathbf{(k)} + \beta_1\mathbf{e_{rr}(k)} \\ \widehat{\mathbf{D_{dq1}}}\mathbf{(k+1)} = \beta_2\mathbf{e_{rr}(k)} + \widehat{\mathbf{D_{dq1}}}\mathbf{(k)} \end{cases} \tag{4}$$

β_1, β_2 denote the LDO coefficients; $\widehat{\mathbf{i_{dq}}} = \begin{bmatrix} \widehat{i_d} \\ \widehat{i_q} \end{bmatrix}$; $\widehat{\mathbf{D_{dq1}}} = \begin{bmatrix} \widehat{D_{d1}} \\ \widehat{D_{q1}} \end{bmatrix}$; $\widehat{D_{d1}}, \widehat{D_{q1}}$ mean the dq-axis disturbances from LDO, respectively.

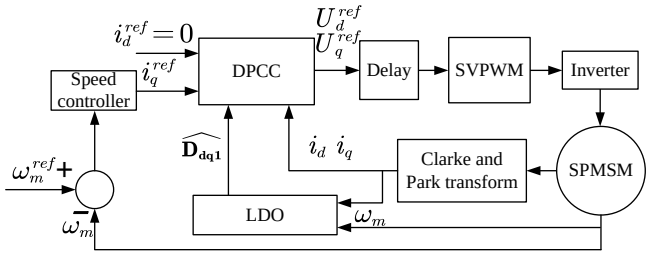

Fig. 2. Block diagram of the DPCC with LDO.

2) After obtaining the total disturbances at the kth and (k+1)th instant, the (k+1)th instant reference voltage can be easily obtained as follows:

$$\begin{cases} \mathbf{i_{dq}(k+1)} = \mathbf{i_{dq}(k)} + \dfrac{T_s}{L_{s0}}\mathbf{U_{dq}^{ref}(k)} + \widehat{\mathbf{D_{dq1}}}\mathbf{(k)} \\ \mathbf{U_{dq}^{ref}(k+1)} = \dfrac{L_{s0}}{T_s}[\mathbf{i_{dq}^{ref}(k)} - \mathbf{i_{dq}(k+1)} - \widehat{\mathbf{D_{dq1}}}\mathbf{(k+1)}] \end{cases} \tag{5}$$

The block diagram of the DPCC with LDO is presented in Fig.2.

III. Limitation of the Conventional DPCC with LDO

Although the conventional DPCC with LDO owns the fast dynamic response and can suppress disturbances based on LDO, several limitations of the DPCC with LDO for becoming high performance current controllers exist, which are clarified in this section.

Defining the actual total disturbances as $\mathbf{D_{dq1}}$, the SPMSM voltage equations can be rewritten based on (1) as follows:

$$\frac{d\mathbf{i_{dq}}}{dt} = \frac{\mathbf{U_{dq}^{ref}}}{L_s} + \frac{\mathbf{D_{dq1}}}{T_s} \tag{6}$$

where $\mathbf{D_{dq1}} = \begin{bmatrix} -\frac{R_s i_d T_s}{L_s} - \frac{U_d^{'} T_s}{L_s} + \omega_e i_q T_s \\ -\frac{R_s i_q T_s}{L_s} - \frac{U_q^{'} T_s}{L_s} - \frac{\psi_m \omega_e(k) T_s}{L_s} - \omega_e i_d T_s \end{bmatrix}$.

Considering current measurement noises $\sigma_{\mathbf{dq}}$, the measured stator current can be expressed as $\mathbf{i_{dq}} + \sigma_{\mathbf{dq}}$. In this case, the LDO equations can be reconstructed as follows:

$$\begin{cases} \dfrac{d\widehat{\mathbf{i_{dq}}}}{dt} = \dfrac{\mathbf{U_{dq}^{ref}}}{L_{s0}} + \dfrac{\widehat{\mathbf{D_{dq1}}}}{T_s} + \dfrac{\beta_1}{T_s}\mathbf{e_{rr}} - \dfrac{\beta_1}{T_s}\sigma_{\mathbf{dq}} \\ \dfrac{d\widehat{\mathbf{D_{dq1}}}}{dt} = \dfrac{\beta_2}{T_s}\mathbf{e_{rr}} - \dfrac{\beta_2}{T_s}\sigma_{\mathbf{dq}} \\ \mathbf{e_{rr}} = \widehat{\mathbf{i_{dq}}} - \mathbf{i_{dq}} \end{cases} \tag{7}$$

Subtracting (6) with (7), the estimated disturbance equations can be constructed as follows:

$$\begin{cases} \dfrac{d\mathbf{e_{rr}}}{dt} = (\dfrac{1}{L_{s0}} - \dfrac{1}{L_s})\mathbf{U_{dq}^{ref}} + \dfrac{\widehat{\mathbf{D_{dq1}}} - \mathbf{D_{dq1}}}{T_s} + \dfrac{\beta_1}{T_s}\mathbf{e_{rr}} - \dfrac{\beta_1}{T_s}\sigma_{\mathbf{dq}} \\ \dfrac{d\widehat{\mathbf{D_{dq1}}}}{dt} = \dfrac{\beta_2}{T_s}\mathbf{e_{rr}} - \dfrac{\beta_2}{T_s}\sigma_{\mathbf{dq}} \end{cases} \tag{8}$$

In (8), substituting the second equation into the first one, Laplace transform is employed herein, and the estimated disturbance transfer function in s domain is presented as:

$$\frac{\overbrace{\widehat{\mathbf{D_{dq1}}(\mathbf{s})}}^{\text{Term1}}}{T_s s\sigma_{\mathbf{dq}}(\mathbf{s})+(\frac{T_s}{L_s}-\frac{T_s}{L_{s0}})\mathbf{U_{dq}^{ref}}(\mathbf{s})+\mathbf{D_{dq1}}(\mathbf{s})}=\frac{\overbrace{-\frac{\beta_2}{T_s^2}}^{\text{Term2}}}{s^2-\frac{\beta_1}{T_s}s-\frac{\beta_2}{T_s^2}} \tag{9}$$

Regarding to Term2 of (9), it can be seen that Term2 is the second order system transfer function. To avoid the system output overshoot, the value of the damping factor can be set to 1, and β_1, β_2 can be respectively designed as:

$$\begin{cases}\beta_1=-2T_s w_n\\ \beta_2=-T_s^2 w_n^2\end{cases} \tag{10}$$

The total step response disturbance function $r(s)$ can be expressed:

$$r(s)=\frac{k_1}{s}\frac{-\frac{\beta_2}{T_s^2}}{s^2-\frac{\beta_1}{T_s}s-\frac{\beta_2}{T_s^2}}=k_1[\frac{1}{s}-\frac{1}{s+w_n}-\frac{w_n}{(s+w_n)^2}] \tag{11}$$

where k_1 is the magnitude of the step response. Based on the inverse Laplace transform, (11) can be transformed as:

$$r(t)=k_1[1-e^{-w_n t}(1+w_n t)], t\geq 0 \tag{12}$$

From the above equation, it can be seen that the steady state error of the evaluated disturbance transfer function is zero and the convergent speed can be risen with the increase of w_n.

In respect of Term1 of (9), it can be known that the predicted total disturbances $\widehat{\mathbf{D_{dq1}}(\mathbf{s})}$ will track the disturbances $T_s s\sigma_{\mathbf{dq}}(\mathbf{s})+(\frac{T_s}{L_s}-\frac{T_s}{L_{s0}})\mathbf{U_{dq}^{ref}}(\mathbf{s})+\mathbf{D_{dq1}}(\mathbf{s})$, which is rewritten as:

$$\frac{\overbrace{\mathbf{\Delta_{11}}(\mathbf{s})+\mathbf{\Delta_{12}}(\mathbf{s})+\mathbf{\Delta_{13}}(\mathbf{s})}^{\widehat{\mathbf{D_{dq1}}(\mathbf{s})}}}{T_s s\sigma_{\mathbf{dq}}(\mathbf{s})+(\frac{T_s}{L_s}-\frac{T_s}{L_{s0}})\mathbf{U_{dq}^{ref}}(\mathbf{s})+\mathbf{D_{dq1}}(\mathbf{s})}=\frac{w_n^2}{(s+w_n)^2} \tag{13}$$

where the estimated disturbances can be constituted by three parts, i.e., $\mathbf{\Delta_{11}}(\mathbf{s})$ caused by $T_s s\sigma_{\mathbf{dq}}(\mathbf{s})$, $\mathbf{\Delta_{12}}(\mathbf{s})$ caused by $(\frac{T_s}{L_s}-\frac{T_s}{L_{s0}})\mathbf{U_{dq}^{ref}}(\mathbf{s})$ and $\mathbf{\Delta_{13}}(\mathbf{s})$ caused by $\mathbf{D_{dq1}}(\mathbf{s})$. Overall, the limitations of the conventional DPCC with LDO are summarized in the following three factors, i.e., (i) Current measurement noises limitation caused by $T_s s\sigma_{\mathbf{dq}}(\mathbf{s})$; (ii) Initial inductance parameter mismatch limitation caused by $(\frac{T_s}{L_s}-\frac{T_s}{L_{s0}})\mathbf{U_{dq}^{ref}}(\mathbf{s})$; (iii) High frequency disturbances limitation caused by $\mathbf{D_{dq1}}(\mathbf{s})$.

A. Current Measurement Noises Limitation

In practical systems, current measurement noises $\sigma_{\mathbf{dq}}$ generally can be divided into quantization noise and electromagnetic interference (EMI) noise. The quantization and EMI noises contain different magnitudes of high frequency components. The frequency and magnitude of the noises are depended on PWM control period, current sampling resolution from sensor, electrical angular speed, etc. The evaluated disturbance $\mathbf{\Delta_{11}}$ caused by the current measurement noises based on (13) can be expressed as:

$$\mathbf{\Delta_{11}}(\mathbf{s})=\frac{w_n^2}{(s+w_n)^2}T_s s\sigma_{\mathbf{dq}}(\mathbf{s}) \tag{14}$$

It can be seen that the derivative term of $\sigma_{\mathbf{dq}}$ exists and hence the high frequency noises components can be further amplified. The evaluated disturbance $\mathbf{\Delta_{11}}$ caused by the current measurement noises can be enhanced with the increase of w_n and the DPCC with LDO performance will be deteriorated based on (5). As a result, the disturbance rejection of the PCC with LDO can be limited by the magnitude of current measurement noises. It is a trade-off for w_n selection in the DPCC with LDO.

B. Initial Inductance Parameter Mismatch Limitation

When the initial inductance parameter mismatch condition, i.e., $L_{s0}\neq L_s$ occurs in the DPCC with LDO, the evaluated disturbance $\mathbf{\Delta_{12}}$ caused by $L_{s0}\neq L_s$ based on (13) can be presented as:

$$\mathbf{\Delta_{12}}(\mathbf{s})=\frac{w_n^2}{(s+w_n)^2}(\frac{T_s}{L_s}-\frac{T_s}{L_{s0}})\mathbf{U_{dq}^{ref}}(\mathbf{s}) \tag{15}$$

Ideally, if $\mathbf{U_{dq}^{ref}}(\mathbf{s})$ only contains the low frequency or constant voltage, the following term can be satisfied: $\mathbf{\Delta_{12}}(\mathbf{s})=(\frac{T_s}{L_s}-\frac{T_s}{L_{s0}})\mathbf{U_{dq}^{ref}}(\mathbf{s})$ at steady state. Substituting $\mathbf{\Delta_{12}}(\mathbf{s})=(\frac{T_s}{L_s}-\frac{T_s}{L_{s0}})\mathbf{U_{dq}^{ref}}(\mathbf{s})$ into (5), the (k+1)th instant reference voltage can be rearranged as:

$$\begin{cases}\mathbf{i_{dq}}(\mathbf{k+1})=\mathbf{i_{dq}}(\mathbf{k})+\frac{T_s}{L_s}\mathbf{U_{dq}^{ref}}(\mathbf{k})+\mathbf{\Delta_{11}}(\mathbf{k})+\mathbf{\Delta_{13}}(\mathbf{k})\\ \mathbf{U_{dq}^{ref}}(\mathbf{k+1})=\frac{L_s}{T_s}[\mathbf{i_{dq}^{ref}}(\mathbf{k})-\mathbf{i_{dq}}(\mathbf{k+1})-\mathbf{\Delta_{11}}(\mathbf{k+1})\\ \qquad\qquad -\mathbf{\Delta_{13}}(\mathbf{k+1})]\end{cases} \tag{16}$$

From the above equations, it can be seen that the initial inductance parameter L_{s0} is removed in (16) and the DPCC with LDO seemingly can not be affected under the initial inductance parameter mismatch. However, $\mathbf{U_{dq}^{ref}}(\mathbf{s})$ cannot be accurately obtained by LDO mainly because $\mathbf{U_{dq}^{ref}}(\mathbf{s})$ contains the derivative term of stator currents based on (1) and the derivative term can induce much more high frequency components. In this case, the term $\mathbf{\Delta_{12}}(\mathbf{s})\neq(\frac{T_s}{L_s}-\frac{T_s}{L_{s0}})\mathbf{U_{dq}^{ref}}(\mathbf{s})$ will occur in practical systems and the DPCC with LDO performance will be deteriorated under $L_{s0}\neq L_s$.

C. High Frequency Disturbance Limitation

The evaluated disturbance $\mathbf{\Delta_{13}}$ caused by $\mathbf{D_{dq1}}$ based on (13) can be presented as:

$$\mathbf{\Delta_{13}}(\mathbf{s})=\frac{w_n^2}{(s+w_n)^2}\mathbf{D_{dq1}}(\mathbf{s}) \tag{17}$$

According to (6), it can be seen that $\mathbf{D_{dq1}}$ can be categorized into the inverter disturbance $U_d^{'}$, $U_q^{'}$ and SPMSM parameter mismatch disturbance.

The actual distorted voltage $U_\alpha^{'}$ and $U_\beta^{'}$ caused by inverter nonlinearity can be obtained by the inverter model, which can be presented as follows [17]:

$$\begin{cases} U_\alpha^{'} = \widehat{U}[2sign(i_a) - sign(i_b) - sign(i_c)] \\ U_\beta^{'} = \widehat{U}[\sqrt{3}sign(i_b) - \sqrt{3}sign(i_c)] \\ \widehat{U} = \dfrac{1}{3}[(V_{dc} - V_{ce} + V_d)\dfrac{t_d + t_{on} - t_{off}}{T_s} + \dfrac{V_{ce0} + V_{d0}}{2}] \end{cases} \tag{18}$$

where $\widehat{U}$ is the amplitude of the distorted voltage; i_a, i_b, i_c are the SPMSM A, B and C phases stator currents, respectively; V_{ce}, V_d are the voltage drop of the active switch and free-wheeling diode; V_{dc} is the dc bus voltage; t_d, t_{on}, t_{off} are the system deadtime, turn-on time delay and turn-off time delay; V_{ce0}, V_{d0} are the threshold voltages of the active switch and freewheeling diode; The symbol $sign$ is the signum function. It can be seen that the frequency of the distorted voltage $U_d^{'}$ and $U_q^{'}$ caused by inverter nonlinearity is proportional to the machine speed, i.e., $U_d^{'} = U_\alpha^{'}cos\theta_e + U_\beta^{'}sin\theta_e$ and $U_q^{'} = -U_\alpha^{'}sin\theta_e + U_\beta^{'}cos\theta_e$. In this case, the sixth order high frequency $U_d^{'}$ and $U_q^{'}$ harmonic is generated by the inverter disturbance. According to (17), LDO cannot evaluate the disturbance under relatively high speed condition[1]. $w_n < 6\omega_e$ under relatively high speed condition since w_n is limited by the current measurement noises and hence the actual inverter disturbance cannot be accurately evaluated. To illustrate the theoretical correctness, the experimental and theoretical results of estimated $U_\alpha^{'}$ and $U_\beta^{'}$ from LDO are shown in Fig.3. The dotted line is the theoretical result of the evaluated inverter disturbance based on (18) while the solid line is the experimental result of the evaluated inverter disturbance from LDO. It can be seen that the estimated disturbances $U_\alpha^{'}$ and $U_\beta^{'}$ from LDO are approximately consistent with that of the theoretical results under low speed 100rpm speed condition whereas the large variation of the estimated disturbances between experimental and theoretical results occurs when the SPMSM speed is increased to 1000rpm speed condition. Overall, the inverter parameter disturbances $U_d^{'}$ and $U_q^{'}$ under relatively high speed condition belong to high frequency disturbances and can not be obtained from LDO.

Because the resistance, inductance and rotor flux linkage parameters can not vary fast due to SPMSM property, the terms $\frac{R_s i_d T_s}{L_s}, \frac{R_s i_q T_s}{L_s}, \frac{\psi_m \omega_e(k) T_s}{L_s}$ in $\mathbf{D_{dq1}}$ can be accurately obtained by LDO. The value of d-axis current is taken as zero below the SPMSM rated speed condition and the current cannot change fast under flux-weakening region while the q-axis is proportional to the electromagnetic torque. It can be known that a sudden q-axis reference current usually happens in SPMSM drive applications, i.e. torque control in electric vehicles. The step q-axis reference current can force the fast variation of q-axis stator currents, which can induce the high frequency disturbance caused by $\frac{R_s i_q T_s}{L_s}$ in $\mathbf{D_{dq1}}$. In addition, the disturbance caused by $\omega_e i_q T_s$ under the sudden q-axis reference current can generate much more high frequency components. Therefore, it is a limitation for LDO to estimate the disturbance caused by $\frac{R_s i_q T_s}{L_s}, \omega_e i_q T_s$ in $\mathbf{D_{dq1}}$ under the sudden q-axis reference current, i.e., $\mathbf{\Delta_{13}} \neq \mathbf{D_{dq1}}$ at steady state under the sudden q-axis reference current.

[1]Since 1500rpm is the SPMSM rated speed and the above 1000rpm speed condition can be considered as relatively high speed condition in this paper.

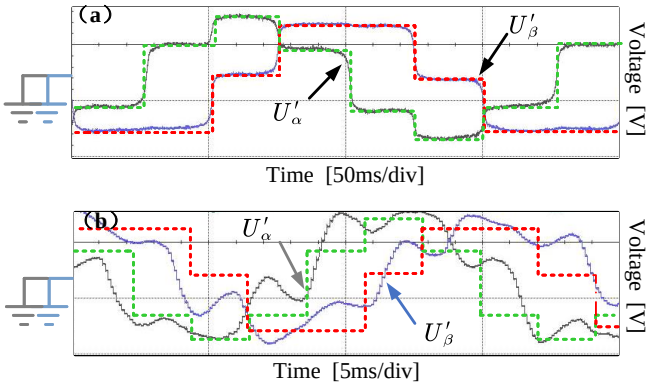

Fig. 3. Experimental and theoretical results of the estimated inverter voltage disturbances. (a) 100rpm speed condition; (b) 1000rpm speed condition.

IV. Proposed DPCC with LDO

In order to enhance the DPCC with LDO performance and suppress the most parts of the limitations effect on the DPCC with LDO, an enhanced DPCC with LDO is proposed in this section. The SPMSM voltage equation can be reconstructed as:

$$\frac{d\mathbf{i_{dq}}}{dt} = \frac{\mathbf{U_{dq}^{ref}} - \mathbf{U_{dq}^{'}}}{L_s} + \frac{\mathbf{D_{dq2}}}{T_s} + \frac{\mathbf{G}}{T_s} \tag{19}$$

where $\mathbf{G} = \begin{bmatrix} \omega_e i_q T_s \\ -\omega_e i_d T_s \end{bmatrix}$, $\mathbf{D_{dq2}} = \begin{bmatrix} -\frac{R_s i_d T_s}{L_s} \\ -\frac{R_s i_q T_s}{L_s} - \frac{\psi_m \omega_e T_s}{L_s} \end{bmatrix}$. It should be noted that some disturbances in $\mathbf{D_{dq1}}$ is taken as known variables as shown in $\mathbf{G}$ and $\mathbf{U_{dq}^{'}}$. Compared with $\mathbf{D_{dq1}}$, the effect of the high frequency disturbances caused by inverter nonlinearty and abrupt $\mathbf{G}$ on LDO can be eliminated. The proposed DPCC with LDO mainly consists of three parts, i.e., the proposed LDO, inductance and inverter disturbance observer and DPCC based on (19). The detailed procedure of proposed DPCC with LDO and inductance and inveter disturbance observer will be presented in subsection-A and B. Furthermore, the proposed DPCC with LDO performance evaluation will be analyzed in subsection-C.

A. Design of Proposed DPCC with LDO

The proposed LDO is designed as follows:

$$\begin{cases} \dfrac{d\widehat{\mathbf{i_{dq}}}}{dt} = \dfrac{\mathbf{U_{dq}^{ref}} - \widehat{\mathbf{U_{dq}^{'}}}}{\widehat{L}} + \dfrac{\widehat{\mathbf{D_{dq2}}}}{T_s} + \dfrac{\mathbf{G}}{T_s} + \dfrac{\gamma_2}{T_s}\chi \\ \dfrac{d\widehat{\mathbf{D_{dq2}}}}{dt} = \dfrac{\gamma_3}{T_s}\chi \\ \dfrac{d\chi}{dt} = \mathbf{e_{rr}} - \gamma_1\chi \\ \mathbf{e_{rr}} = \widehat{\mathbf{i_{dq}}} - \mathbf{i_{dq}} \end{cases} \tag{20}$$

where $\widehat{\mathbf{D_{dq2}}} = \begin{bmatrix} \widehat{D_{d2}} \\ \widehat{D_{q2}} \end{bmatrix}$; $\widehat{D_{d2}}, \widehat{D_{q2}}$ mean the dq-axis disturbances from the proposed LDO, respectively; $\gamma_1, \gamma_2, \gamma_3$ denote

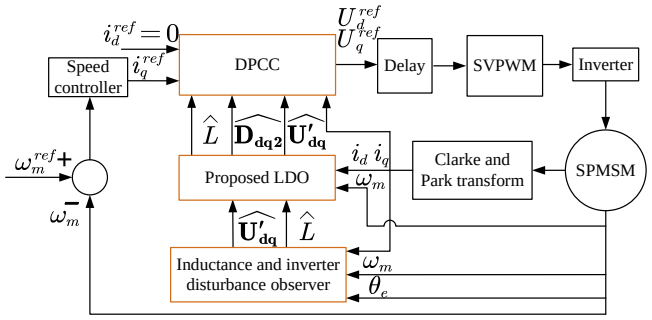

Fig. 4. Block diagram of the proposed DPCC with LDO.

the proposed LDO coefficients. It should be noted that L_{s0} and $\mathbf{U}'_{\mathbf{dq}}$ can be acquired from the proposed inductance and inverter disturbance observer, and hence the predicted $\widehat{L}$ and $\widehat{\mathbf{U}'_{\mathbf{dq}}}$ from the proposed observer will respectively replace L_{s0} and $\mathbf{U}'_{\mathbf{dq}}$. The digital implementation of the proposed LDO can be presented as follows:

$$\begin{cases} \mathbf{e_{rr}(k)} = \widehat{\mathbf{i_{dq}}}(\mathbf{k}) - \mathbf{i_{dq}(k)} \\ \widehat{\mathbf{i_{dq}}}(\mathbf{k+1}) = \widehat{\mathbf{i_{dq}}}(\mathbf{k}) + \dfrac{T_s}{\widehat{L}(k)}[\mathbf{U^{ref}_{dq}}(\mathbf{k}) - \widehat{\mathbf{U}'_{\mathbf{dq}}}(\mathbf{k})] + \mathbf{G(k)} \\ \qquad\qquad + \widehat{\mathbf{D_{dq2}}}(\mathbf{k}) + \gamma_2\chi(\mathbf{k}) \\ \widehat{\mathbf{D_{dq2}}}(\mathbf{k+1}) = \gamma_3\chi(\mathbf{k}) + \widehat{\mathbf{D_{dq2}}}(\mathbf{k}) \\ \chi(\mathbf{k}) = \dfrac{1}{1+T_s\gamma_1}\left[T_s\mathbf{e_{rr}(k)} + \chi(\mathbf{k-1})\right] \end{cases} \tag{21}$$

After obtaining the total disturbances $\widehat{\mathbf{D_{dq2}}}$, the (k+1)th instant reference voltage can be obtained as follows:

$$\begin{cases} \mathbf{i_{dq}(k+1)} = \mathbf{i_{dq}(k)} + \dfrac{T_s}{\widehat{L}(k)}[\mathbf{U^{ref}_{dq}}(\mathbf{k}) - \widehat{\mathbf{U}'_{\mathbf{dq}}}(\mathbf{k})] \\ \qquad\qquad + \mathbf{G(k)} + \widehat{\mathbf{D_{dq2}}}(\mathbf{k}) \\ \mathbf{U^{ref}_{dq}(k+1)} = \dfrac{\widehat{L}(k+1)}{T_s}[\mathbf{i^{ref}_{dq}}(\mathbf{k}) - \mathbf{i_{dq}(k+1)} - \mathbf{G(k+1)} \\ \qquad\qquad - \widehat{\mathbf{D_{dq2}}}(\mathbf{k+1})] + \widehat{\mathbf{U}'_{\mathbf{dq}}}(\mathbf{k+1}) \end{cases} \tag{22}$$

The block diagram of the proposed DPCC with LDO is presented in Fig.4.

B. Design of Inductance and Inverter Disturbance Observer

In order to obtaining the predicted $\widehat{L}$ and $\widehat{\mathbf{U}'_{\mathbf{dq}}}$, a non-invasive inductance and inverter disturbance observer is proposed.

1) Selection of Inductance and Distorted Voltage Observer Region: The SPMSM voltage equation on β-axis and d-axis frame can be expressed as follows:

$$\begin{cases} U_\beta^{ref} = R_s i_\beta + L_s\dfrac{di_\beta}{dt} + \omega_e\psi_m cos\theta_e + U'_\beta \\ U_d^{ref} = L_s\dfrac{di_d}{dt} + R_s i_d - \omega_e L_s i_q + U'_d \end{cases} \tag{23}$$

where U_β^{ref} is the inverter output reference voltage on β-axis. Since the SPMSM stator current vector position is 90 degree

TABLE I
RELATIONSHIP BETWEEN θ_e AND INVERTER DISTURBANCE

Region	θ_e	U'_α	U'_β	U'_d	U'_q
I	$\frac{8\pi}{6} \sim \frac{10\pi}{6}$	$4\widehat{U}$	0	$\widehat{U}cos(\theta_e - \frac{\pi}{2})$	$-\widehat{U}sin\theta_e$
II	$\frac{10\pi}{6} \sim \frac{12\pi}{6}$	$2\widehat{U}$	$2\sqrt{3}\widehat{U}$	$\widehat{U}cos(\theta_e - \frac{5\pi}{6})$	$-\widehat{U}sin(\theta_e - \frac{5\pi}{6})$
III	$\frac{0\pi}{6} \sim \frac{2\pi}{6}$	$-2\widehat{U}$	$2\sqrt{3}\widehat{U}$	$-\widehat{U}cos(\theta_e - \frac{\pi}{6})$	$\widehat{U}sin(\theta_e - \frac{\pi}{6})$
IV	$\frac{2\pi}{6} \sim \frac{4\pi}{6}$	$-4\widehat{U}$	0	$-\widehat{U}cos(\theta_e - \frac{\pi}{2})$	$\widehat{U}sin(\theta_e - \frac{\pi}{2})$
V	$\frac{4\pi}{6} \sim \frac{6\pi}{6}$	$-2\widehat{U}$	$-2\sqrt{3}\widehat{U}$	$-\widehat{U}cos(\theta_e - \frac{5\pi}{6})$	$\widehat{U}sin(\theta_e - \frac{5\pi}{6})$
VI	$\frac{6\pi}{6} \sim \frac{8\pi}{6}$	$2\widehat{U}$	$-2\sqrt{3}\widehat{U}$	$\widehat{U}cos(\theta_e - \frac{\pi}{6})$	$-\widehat{U}sin(\theta_e - \frac{\pi}{6})$

TABLE II
INDUCTANCE AND INVERTER DISTURBANCE OBSERVER REGION WITH θ_e

Region	θ_e	U'_α	U'_β	Region	θ_e	U'_α	U'_β
A	$\frac{9\pi}{6} - \delta_1 \sim \frac{9\pi}{6} + \delta_1$	$4\widehat{U}$	0	**D**	$\frac{9\pi}{6} + \delta_2 \sim \frac{10\pi}{6} - \delta_2$	$4\widehat{U}$	0
B	$\frac{3\pi}{6} - \delta_1 \sim \frac{3\pi}{6} + \delta_1$	$-4\widehat{U}$	0	**E**	$\frac{2\pi}{6} + \delta_2 \sim \frac{3\pi}{6} - \delta_2$	$-4\widehat{U}$	0
C	$\frac{8\pi}{6} + \delta_2 \sim \frac{9\pi}{6} - \delta_2$	$4\widehat{U}$	0	**F**	$\frac{3\pi}{6} + \delta_2 \sim \frac{4\pi}{6} - \delta_2$	$-4\widehat{U}$	0

ahead of the SPMSM electrical angle θ_e, the relationship between θ_e and the inverter disturbance can be presented in TABLE.I. When θ_e is located in region I and IV of TABLE.I, (23) can be reconstructed as:

$$\begin{cases} U_\beta^{ref} = \overbrace{(R_s i_q + L_s\dfrac{di_q}{dt} + \omega_e\psi_m)cos\theta_e}^{\text{Term3}} - \overbrace{\omega_e i_q L_s sin\theta_e}^{\text{Term4}} \\ U_d^{ref} = U'_\alpha cos\theta_e - \omega_e i_q L_s \end{cases} \tag{24}$$

Based on the above equation, the inductance and inverter disturbance observer region is further developed in TABLE.II, where δ_1 is the tuned coefficient and is set to $\frac{\pi}{180}$ to obtain the inductance identification in this paper. The reason for the value of $\frac{\pi}{180}$ selection is that the amplitude of $\sin(\frac{3\pi}{6} \pm \frac{\pi}{180}) \approx 0.9998476$ and the amplitude of $\sin(\frac{9\pi}{6} \pm \frac{\pi}{180}) \approx 0.9998476$ is much 50 times larger than the amplitude of $\cos(\frac{3\pi}{6} \pm \frac{\pi}{180}) \approx 0.0174524$ and $\cos(\frac{9\pi}{6} \pm \frac{\pi}{180}) \approx 0.0174524$. Therefore, the value of Term3 in (24) is much smaller and can be neglected compared with Term4 at steady state. With the decrease of the value of δ_1, the proposed observer needs more time for the inductance identification. δ_2 is another tuned coefficient and the value selection is based on different types of inverters. The range of δ_2 is $(0, \frac{\pi}{6})$ and the smaller the value is chosen, the slower the estimated speed is.

2) Design of Inductance and Inverter Disturbance Observer: Based on the above analysis, the inductance and inverter disturbance model (the proposed plant model) can be designed as:

$$\begin{cases} \widehat{U_\beta^{ref}} = -\omega_e i_q \widehat{L} sin\theta_e & \theta_e \in (\mathbf{A}, \mathbf{B}) \\ \widehat{U_d^{ref}} = 4\xi cos\theta_e \widehat{U} - \omega_e i_q \widehat{L} & \theta_e \in (\mathbf{C}, \mathbf{D}, \mathbf{E}, \mathbf{F}) \end{cases} \tag{25}$$

where $\xi = 1$ and $\xi = -1$ are in regions $\mathbf{C}, \mathbf{D}$ and $\mathbf{E}, \mathbf{F}$, respectively; $\widehat{U_\beta^{ref}}$ is the β-axis predicted inverter output reference voltage; $\widehat{U_d^{ref}}$ is the d-axis predicted inverter output reference voltage. Utilizing the internal model control principle, the predicted inverter output reference voltages $\widehat{U_\beta^{ref}}(s)$ and $\widehat{U_d^{ref}}(s)$ are considered as output variables of the plant model, while the predicted $\widehat{L}(s)$ and $\widehat{U}(s)$ are taken as input variables of the

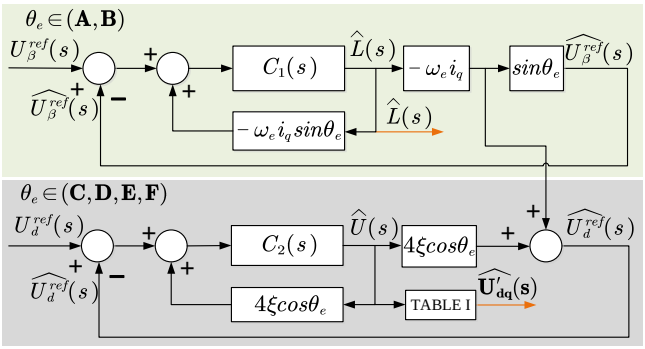

Fig. 5. Block diagram of the inductance and inverter disturbance observer.

plant model. Meanwhile, the term $-\omega_e i_q(s)\widehat{L}(s)$ is considered as external disturbances of the plant model. The block diagram of the inductance and inverter disturbance observer is shown in Fig.5. The internal model controller transfer function $C_1(s)$ and $C_2(s)$ can be respectively expressed as:

$$\begin{cases} C_1(s) = -\dfrac{1}{\omega_e i_q sin\theta_e} Z(s) \\ C_2(s) = \dfrac{1}{4\xi cos\theta_e} Z(s) \\ Z(s) = \dfrac{2\pi f_{b2}}{s + 2\pi f_{b2}} \end{cases} \tag{26}$$

where f_{b2} is the observer bandwidth. In order to get a fast, zero steady state and stable observer system, $Z(s)$ can be simply chosen as the first order inertia. With the increase of f_{b2}, the observer speed is enhanced, but the high frequency noise will be amplified. It can be noticeable that there are no SPMSM resistance and rotor flux linkage parameters involved and the only known variables are the measured SPMSM electrical angular speed, electrical angle and stator q-axis current, which can be obtained based on position and current sensors. When the proposed inductance and inverter disturbance observer is at steady state, the values of the predicted $\widehat{L}$ and $\widehat{\mathbf{U}'_{\mathbf{dq}}}$ can be approximately equal to the values of the L_s and $U_d^{'}, U_q^{'}$, respectively.

Employing the first-order forward Euler discretization, the (k+1)th instant predicted inductance in regions $\mathbf{A}, \mathbf{B}$ can be obtained as follows:

$$\begin{cases} \widehat{U_\beta^{ref}}(k) = -\omega_e(k) i_q(k) sin\theta_e(k) \widehat{L}(k) \\ e_\beta(k) = U_\beta^{ref}(k) - \widehat{U_\beta^{ref}}(k) \\ \widehat{L}(k+1) = \widehat{L}(k) - \dfrac{2\pi f_{b2} T_s e_\beta(k)}{\omega_e(k) sin\theta_e(k) i_q(k)} \end{cases} \tag{27}$$

In regions $\mathbf{C}, \mathbf{D}, \mathbf{E}, \mathbf{F}$, the (k+1)th instant predicted inverter $\widehat{U}$ can be obtained as follows:

$$\begin{cases} \widehat{U_d^{ref}}(k) = 4\xi cos\theta_e(k) \widehat{U}(k) - \omega_e(k) i_q(k) \widehat{L}(k) \\ e_d(k) = U_d^{ref}(k) - \widehat{U_d^{ref}}(k) \\ \widehat{U}(k+1) = \widehat{U}(k) - \dfrac{\pi f_{b2} T_s e_d(k)}{2\xi cos\theta_e(k)} \end{cases} \tag{28}$$

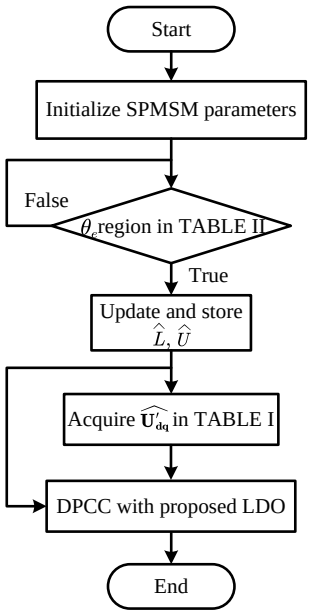

Fig. 6. Flow chart of the proposed DPCC with LDO.

After obtaining $\widehat{U}$, the inverter disturbance $\widehat{\mathbf{U}'_{\mathbf{dq}}}$ can be acquired by TABLE. I. The flow chart of the proposed DPCC with LDO has been shown in Fig.6.

C. Proposed DPCC with LDO Performance Evaluation

Based on (19)-(20), considering current measurement noises $\sigma_{\mathbf{dq}}$, the estimated disturbance equation $\mathbf{F(s)}$ of the proposed DPCC with LDO in s domain is presented as:

$$\begin{cases} \dfrac{\widehat{\mathbf{D}_{\mathbf{dq2}}}(\mathbf{s})}{T_s s \sigma_{\mathbf{dq}}(\mathbf{s}) + T_s[\frac{\mathbf{U_{dq}^{ref}(s)} - \mathbf{U'_{dq}(s)}}{L_s} - \frac{\mathbf{U_{dq}^{ref}(s)} - \widehat{\mathbf{U'_{dq}(s)}}}{\widehat{L}}] + \mathbf{D_{dq2}(s)}} = \mathbf{F(s)} \\ \mathbf{F(s)} = \dfrac{-\frac{\gamma_3}{T_s^2}}{s^3 + \gamma_1 s^2 - \frac{\gamma_2}{T_s} s - \frac{\gamma_3}{T_s^2}} \end{cases} \tag{29}$$

Similarly, the proposed LDO coefficients γ_1, γ_2, and γ_3 can be designed as:

$$\begin{cases} \gamma_1 = 3w_n \\ \gamma_2 = -3T_s w_n^2 \\ \gamma_3 = -T_s^2 w_n^3 \end{cases} \tag{30}$$

Therefore, the estimated disturbance transfer function $\mathbf{F(s)}$ can be expressed as $\mathbf{F(s)} = \frac{w_n^3}{(s+w_n)^3}$. From the transfer function, it can be known that the proposed LDO is stable and steady state error is zero. The LDO convergent speed is increased as the value of w_n enhancing. It should be noted that according to the-3dB bandwidth definition, the value of w_n of the proposed LDO is different from that in the conventional LDO based on (10) and w_n of the proposed LDO is approximately 1.26 times magnitude than that in the conventional LDO to keep the same

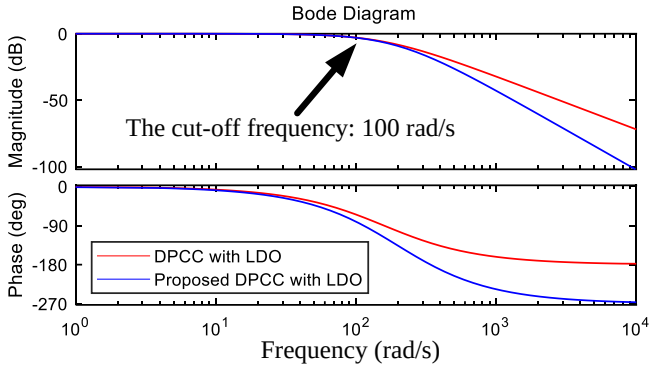

Fig. 7. Bode plot of the two DPCC with LDO under 100rad/s LDO bandwidth.

LDO bandwidth. According to (30), (29) can be rewritten as:

$$\begin{cases} \dfrac{\overbrace{\boldsymbol{\Delta_{21}}(\mathbf{s})+\boldsymbol{\Delta_{22}}(\mathbf{s})+\boldsymbol{\Delta_{23}}(\mathbf{s})}^{\widehat{\mathbf{D}_{\mathbf{dq2}}}(\mathbf{s})}}{T_s s\sigma_{\mathbf{dq}}(\mathbf{s})+T_s[\frac{\mathbf{U}^{\mathbf{ref}}_{\mathbf{dq}}(\mathbf{s})-\mathbf{U}'_{\mathbf{dq}}(\mathbf{s})}{L_s}-\frac{\mathbf{U}^{\mathbf{ref}}_{\mathbf{dq}}(\mathbf{s})-\widehat{\mathbf{U}'_{\mathbf{dq}}(\mathbf{s})}}{\widehat{L}}]+\mathbf{D_{dq2}}(\mathbf{s})}=\mathbf{F}(\mathbf{s}) \\ \mathbf{F}(\mathbf{s})=\dfrac{w_n^3}{(s+w_n)^3} \end{cases} \tag{31}$$

where the estimated disturbances can be constituted by three parts, i.e., $\boldsymbol{\Delta_{21}}(\mathbf{s})$ caused by $T_s s\sigma_{\mathbf{dq}}(\mathbf{s})$, $\boldsymbol{\Delta_{22}}(\mathbf{s})$ caused by $T_s[\frac{\mathbf{U}^{\mathbf{ref}}_{\mathbf{dq}}(\mathbf{s})-\mathbf{U}'_{\mathbf{dq}}(\mathbf{s})}{L_s}-\frac{\mathbf{U}^{\mathbf{ref}}_{\mathbf{dq}}(\mathbf{s})-\widehat{\mathbf{U}'_{\mathbf{dq}}(\mathbf{s})}}{\widehat{L}}]$ and $\boldsymbol{\Delta_{23}}(\mathbf{s})$ caused by $\mathbf{D_{dq2}}(\mathbf{s})$. In order to illustrate the superiority of the proposed DPCC with LDO, three parts of performance evaluation will be carried out, i.e., current measurement noises performance evaluation, initial inductance parameter mismatch performance evaluation and high frequency disturbance performance evaluation.

1) Current Measurement Noises Performance Evaluation: The evaluated disturbance $\boldsymbol{\Delta_{21}}$ caused by the current measurement noises based on (13) can be expressed as:

$$\boldsymbol{\Delta_{21}}(\mathbf{s})=\frac{w_n^3}{(s+w_n)^3}T_s s\sigma_{\mathbf{dq}}(\mathbf{s}) \tag{32}$$

The Bode plot of the conventional DPCC with LDO and proposed DPCC with LDO under the same LDO bandwidth is shown in Fig.7. It can be seen that the evaluated disturbance $\boldsymbol{\Delta_{21}}$ caused by high frequency current measurement noises can be better suppressed in the proposed DPCC with LDO compared with the conventional DPCC with LDO based on (14).

2) Initial Inductance Parameter Mismatch Performance Evaluation: If the inductance parameter and inverter disturbance cannot be acquired, the proposed DPCC with LDO is the same with the conventional DPCC with LDO based on (15). On the contrary, employing the proposed inductance and disturbance observer, $\widehat{L}\approx L_s$ and $\widehat{\mathbf{U}'_{\mathbf{dq}}}\approx\mathbf{U}'_{\mathbf{dq}}$. Therefore, the evaluated disturbance $\boldsymbol{\Delta_{22}}\approx 0$, and the high frequency components of $\mathbf{U}^{\mathbf{ref}}_{\mathbf{dq}}(\mathbf{s})$ cannot affect the proposed DPCC with LDO.

3) High Frequency Disturbance Performance Evaluation: In terms of the inverter disturbance, without employing the start-up and offline inverter nonlinearity commissioning methods, the proposed LDO is able to acquire $\mathbf{U}'_{\mathbf{dq}}$. $\mathbf{D_{dq2}}(\mathbf{s})$ does not include $\mathbf{U}'_{\mathbf{dq}}$, which means that the proposed LDO cannot be affected by the inverter disturbance under high speed condition. In addition, it can be seen that the dq-axis coupling inductance voltage $\mathbf{G}$ is not considered in lumped disturbances and the sudden q-axis reference current cannot affect the proposed LDO on d-axis compared with $\mathbf{D_{dq1}}$. In this case, the high frequency disturbance caused by the sudden q-axis reference current effect on the proposed DPCC with LDO is reduced.

TABLE III
SPMSM AND INVERTER PARAMETERS

Parameters	Value	Unit	Parameters	Value	Unit
Pole pairs (p)	4		Stator inductance (L_d)	5.7	mH
Stator resistance (R_s)	1.12	Ω	Inverter deadtime (t_d)	2.5	μs
Flux linkage (ψ_m)	0.092	Wb	Sampling period (T_s)	100	μs

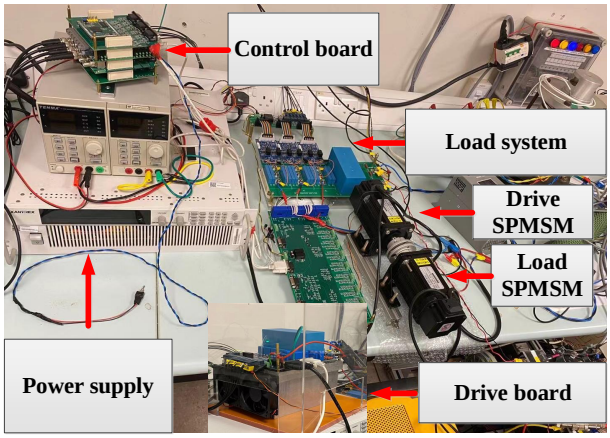

Fig. 8. SPMSM drive test rig.

V. EXPERIMENTAL RESULTS VALIDATION

The SPMSM test rig is constructed as shown in Fig. 8. It includes two XCUBE boards (main control boards), two inverter boards, two SPMSMs, and one main power supply (600V/10A). The SPMSM and inverter parameters are listed in TABLE.III. In order to validate the effectiveness of the proposed DPCC with LDO, four parts of test results will be presented herein, namely proposed inductance and inverter disturbance observer performance evaluation, proposed LDO performance evaluation, proposed DPCC with LDO performance evaluation and calculation time evaluation.

A. Proposed Inductance and Inverter Disturbance Observer Performance Evaluation

Setting the value of the inductance and distorted voltage observer bandwidth f_{b2} and reference d-axis current to 50Hz and 0A, respectively, the proposed observer performance is shown in Fig.9 and Fig.10. The reference q-axis current is set to 4A in Fig.10(a)-(e). In Fig.9(a), it can be seen that twice inductance observer regions ($\mathbf{A}$, $\mathbf{B}$) will occur within one

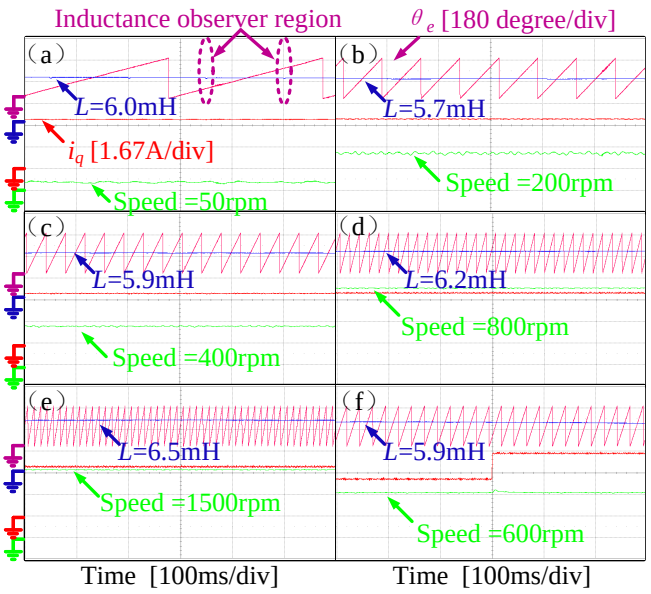

Fig. 9. The estimated inductance performance. (a) 50rpm speed condition; (b) 200rpm speed condition; (c) 400rpm speed condition; (d) 800rpm speed condition; (e) 1500rpm speed condition; (f) The reference q-axis current varies from 3A to 5A under 600rpm speed condition.

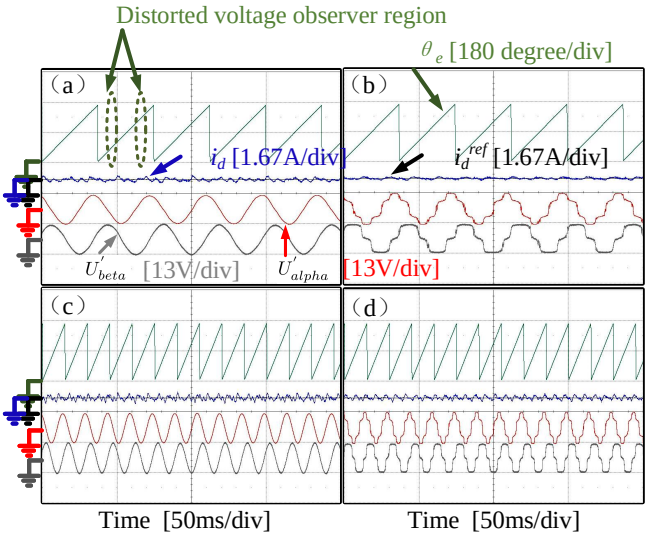

Fig. 10. The d-axis current and estimated distorted voltage comparison under different speed conditions. (a) Conventional DPCC with LDO under 400rpm; (b) Proposed DPCC with LDO under 400rpm; (c) Conventional DPCC with LDO under 1000rpm; (d) Proposed DPCC with LDO under 1000rpm.

SPMSM electrical cycle. The identification region time will be reduced with the SPMSM speed increasing. The maximum variation value of the estimated inductance (6.5mH) under 1500rpm speed condition is quite close to the actual inductance (5.7mH). It should be noted that the small variation between the actual inductance L_s and estimated inductance $\widehat{L}$ can be acceptable since the system exists measurement noises, and 12-bit analogy sampling revolution is applied in the overall system. In order to testify the observer performance at current transient state, it can be seen that the reference q-axis current is abruptly changed from 3A to 5A, but it cannot affect the value of the evaluated inductance in Fig.9(f). Therefore, the

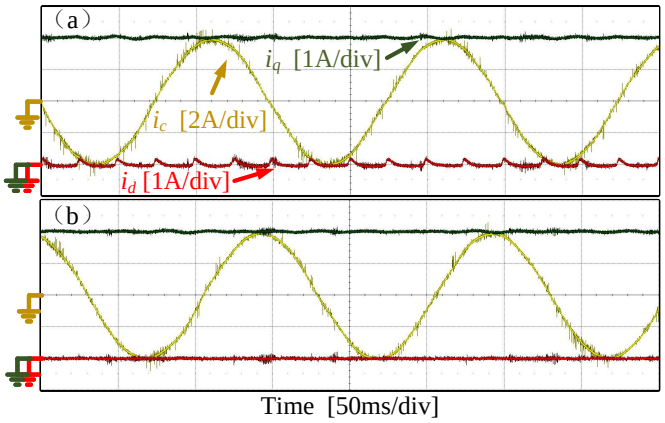

Fig. 11. The current performance under 100rpm speed condition. (a) DPCC with proposed LDO without using inductance and inverter disturbance observer; (b) DPCC with proposed LDO using inductance and inverter disturbance observer.

proposed inductance observer is able to effectively estimate the actual inductance under different conditions.

In order to validate that the proposed observer can accurately evaluate the distorted voltage caused by inverter nonlinearity, the conventional DPCC with LDO based on (4)-(5) and the proposed DPCC with LDO will be made a comparison. The d-axis current and evaluated distorted voltage are shown in Fig.10. In Fig.10(a), it can be seen that the distorted voltage observer regions (**C**, **D**, **E**, **F**) will occur within one electrical cycle. It can be seen the estimated distorted voltage becomes a sine waveform due to the limited LDO bandwidth in Fig.10(a) and Fig.10(c). On the contrary, the estimated distorted voltage from the proposed observer can mainly include the sixth SPMSM electrical frequency component based on (18) in Fig.10(b) and Fig.10(d). Compared with the conventional DPCC with LDO, the d-axis current performance of the proposed DPCC with LDO is improved, which can testify the theoretical correctness of the proposed inductance and inverter disturbance observer.

In addition, the dq-axis and C phase currents performance of the DPCC with proposed LDO using and without using inductance and inverter disturbance observer is shown in Fig.11. Setting the same propose,d LDO cut-off frequency the value of q-axis current keeps 4A, and it can be seen that the DPCC with proposed LDO using inductance and inverter disturbance observer has the better d-axis current performance. The d-axis current of Fig.11(a) has the certain 6th current harmonic and it can be validated that the inductance and inverter disturbance observer can effectively suppress the disturbance caused by inverter nonlinearity while it is difficult for LDO to suppress this type of disturbance. Therefore, it is necessary to employ both LDO and the inductance and inverter disturbance observer into the DPCC scheme.

B. Proposed LDO Performance Evaluation

In order to illustrate the proposed LDO superiority, the conventional LDO based on (4) and proposed LDO based on (21) will be compared in this subsection. The same LDO bandwidth is set in the two LDOs to make a fair comparison

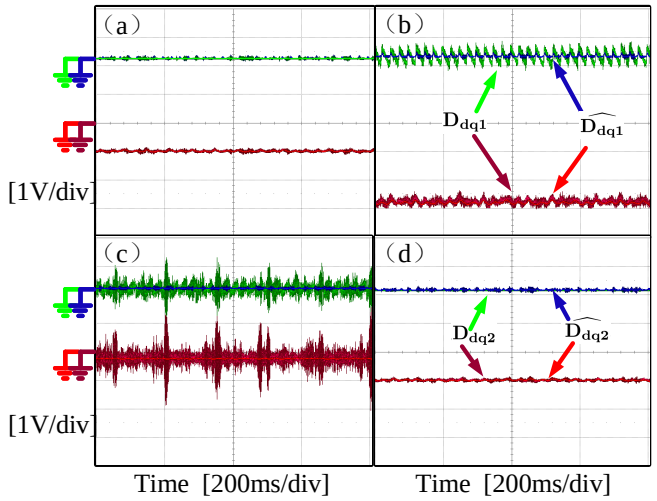

Fig. 12. The disturbances predicted by the two LDOs comparison under 100rpm speed condition. (a) Conventional LDO without inductance mismatch; (b) Conventional LDO under $L_{s0} = 0.5L_s$; (c) Conventional LDO under $L_{s0} = 2L_s$; (d) Proposed LDO.

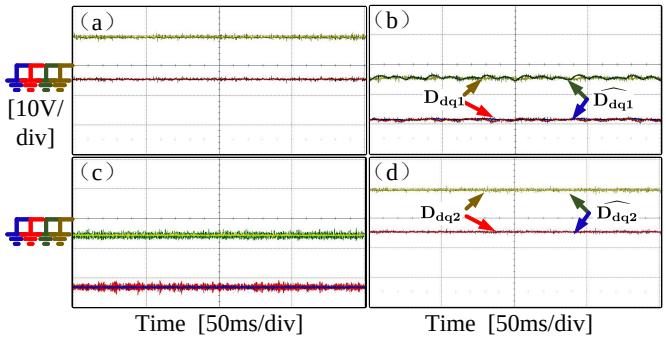

Fig. 13. The disturbances predicted by the two LDOs comparison under 1000rpm speed condition. (a) Conventional LDO without inductance mismatch; (b) Conventional LDO under $L_{s0} = 0.5L_s$; (c) Conventional LDO under $L_{s0} = 1.8L_s$; (d) Proposed LDO.

and the value of the reference dq-axis currents are set to 0A and 2A, respectively. From (6) and (19), it can be known that the actual disturbances of the two LDO are $\mathbf{D_{dq1}}$ and $\mathbf{D_{dq2}}$, respectively. $\mathbf{D_{dq1}}$ and $\mathbf{D_{dq2}}$ can be accurately obtained based on the actual known SPMSM parameters L_s, ψ_m, R_s, measured currents, and SPMSM rotor speed. Since the initial resistance and rotor flux linkage parameters in controller are eliminated in the two LDOs, the disturbances cannot affect the DPCC with LDO. In this case, the estimated disturbances by the two LDOs under SPMSM inductance parameter mismatch condition are carried out in Figs.12-13. It can be seen that the two LDOs performance is almost the same in Figs.12-13(a) and Figs.12-13(d), which can validate the proposed LDO can be immune to the inductance mismatch. When the value of the initial inductance is not equal to the actual inductance, Term1 of (9) includes high frequency noises of $\mathbf{U_{dq}^{ref}}$, and it can negatively affect the DPCC with LDO performance in Figs.12-13(b) and Figs.12-13(c). Based on the above experimental results, it can be seen that the proposed LDO can eliminate the effect of the initial inductance parameter mismatch on the overall system.

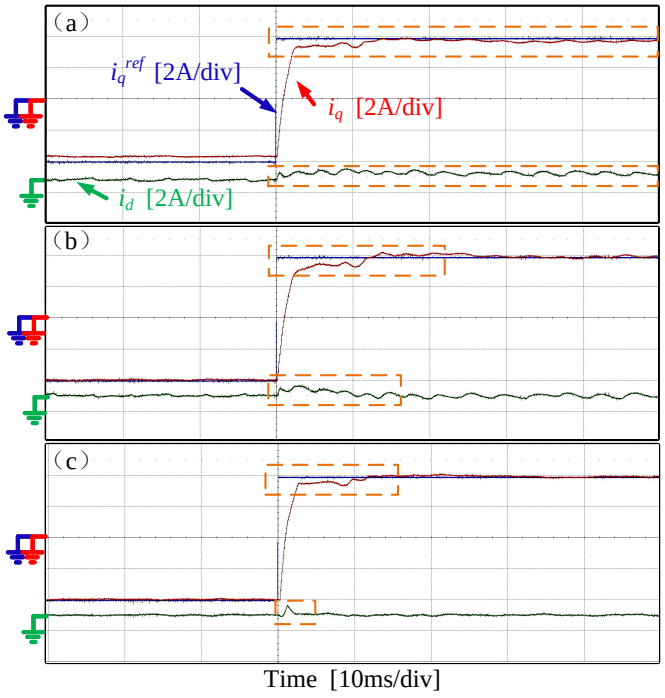

Fig. 14. dq-axis current performance at transient state under 500rpm speed condition. (a) Conventional DPCC under $L_{s0} = 0.5L_s$; (b) Conventional DPCC with LDO under $L_{s0} = 0.5L_s$; (c) Proposed DPCC under $L_{s0} = 0.5L_s$.

C. Proposed DPCC with LDO Performance Evaluation

To validate the proposed DPCC with LDO performance, three methods will be compared, namely the conventional DPCC, conventional DPCC with LDO and proposed DPCC.

First, the dq-axis currents performance at transient state under inductance mismatch conditions will be observed. The value of the q-axis reference current is set from -4A to 4A and the d-axis reference current is set to zero. In Fig.14, it can be seen that when the value of the initial inductance is smaller than the actual inductance, the dynamic response becomes relatively slow and the slight q-axis current overshoot occurs in Fig.14(b), while the best q-axis dynamic response occurs in (c). It can be seen that the dq-axis offset current occurs in Fig.14(a). Due to adding inductance and inverter disturbance observer, the current fluctuation of the proposed DPCC is smallest among the three methods. The q-axis current settling time (within 5 % of its final value) of the three methods is 45ms, 23ms, and 12ms, respectively. The d-axis current settling time of the three methods is 50ms, 6ms, and 2ms, respectively. When the nominal inductance is about two times larger than the actual inductance, the system stability of the DPCC and DPCC with LDO will be deteriorated and the larger current fluctuation will happen, which is the similar test result as shown in Fig.15.

Second, the dq-axis currents performance at steady state under multiple parameters mismatch is carried out to validate the correctness of the proposed DPCC with LDO. Assuming that R_{s0} and ψ_{m0} are the initial nominal resistance and rotor flux linkage parameters in the controller, respectively. The value of the dq-axis current is set to 0A and 4.2A (Rated

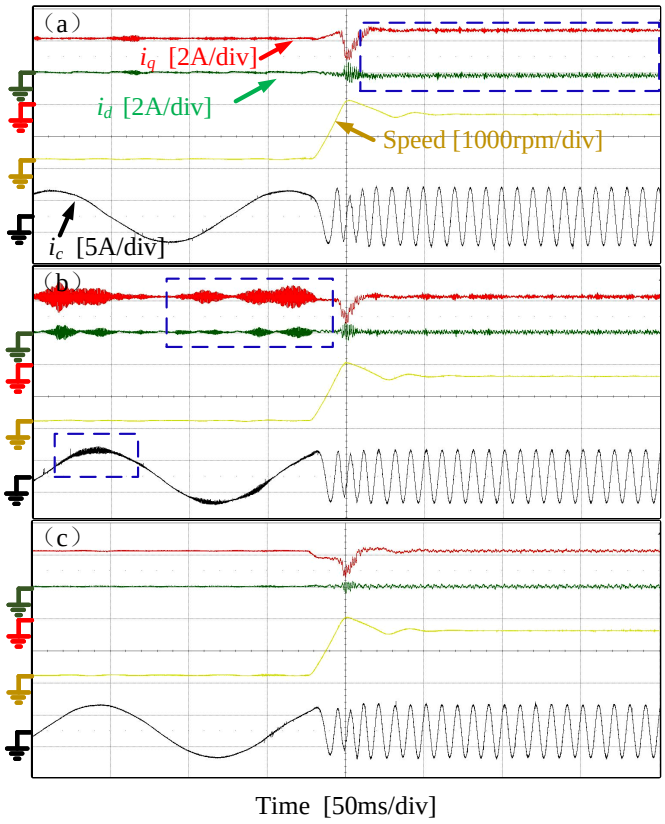

Fig. 15. Three DPCC methods performance comparison. (a), (b) and (c): Conventional DPCC, conventional DPCC with LDO and proposed DPCC under $L_{s0} = 1.85L_s, \psi_{m0} = 1.5\psi_m, R_{s0} = 0.5R_s$ and 100rpm to 1500rpm speed condition.

SPMSM current condition), respectively. In Fig.15, it can be seen that there is a large dc offset in dq-axis current for DPCC while the DPCC with LDO and proposed DPCC with LDO can suppress the disturbances caused by parameter mismatch. Furthermore, it can be seen that the large fluctuation occurs in the DPCC with LDO under this multiple parameters mismatch and the proposed DPCC can own the best current performance under the multiple parameters mismatch. The total harmonic distortion of the three methods is 4.49%, 7.71% and 2.86%, respectively.

Third, when there are only rotor flux linkage and resistance mismatches, the conventional DPCC using inductance and inverter disturbance observer and proposed DPCC are made a comparison as shown in Fig.16. The values of dq-axis currents are set to 0A and 4A, respectively. It can be seen that the rotor flux linkage and resistance mismatch can much influence the q-axis offset current (more than 5A) in the conventional DPCC with inductance and inverter disturbance observer compared with proposed DPCC.

Overall, based on the above current transient and steady experiential results, the proposed DPCC with LDO has the best current performance and is able to suppress the disturbances caused by multiple parameters mismatch and inverter nonlinearity at different conditions.

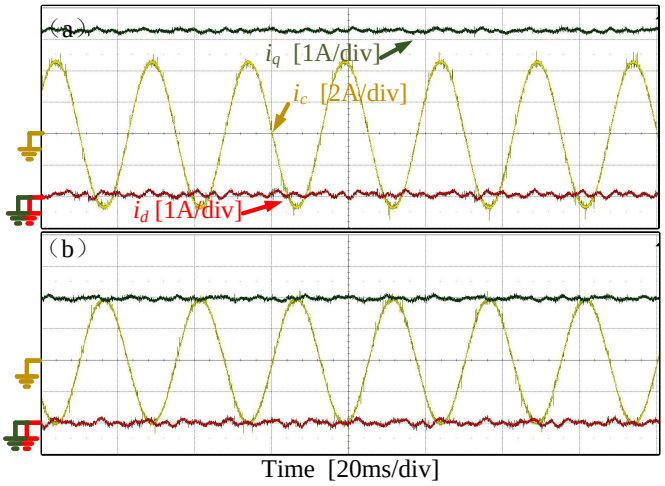

Fig. 16. dq-axis current performance under 600rpm speed condition. (a) Conventional DPCC with inductance and inverter disturbance observer under $\psi_{m0} = 1.5\psi_m, R_{s0} = 2R_s$; (b) Proposed DPCC under $\psi_{m0} = 1.5\psi_m, R_{s0} = 2R_s$.

TABLE IV
COMPUTATION TIME OF THE THREE METHODS

	DPCC	DPCC with LDO	Proposed DPCC
Computation time	17.9 μs	21.3 μs	24.7 μs

D. *Calculation Time Evaluation*

Based on the system clock (200MHZ) of the TMS320F28377 digital signal processor, the calculation burden can be easily evaluated. The computation time of the conventional DPCC, DPCC with LDO and proposed DPCC will be shown in TABLE.IV, respectively. Although the computation time of the proposed DPCC is relatively longer than other methods, it can overcome the initial inductance mismatch effect on DPCC, suppress the disturbance caused by inverter nonlinearity and own the best current performance.

VI. CONCLUSION

In this paper, the limitation of the conventional DPCC with LDO is illustrated. It can be found that the initial inductance parameter, current measurement noises and high frequency disturbance can limit the DPCC with LDO performance. To solve this key issue, an enhanced DPCC with LDO is proposed.

The experimental results have indicated that the proposed inductance and inverter disturbance observer can relatively, accurately estimate the actual inductance and inverter disturbance. Apart from that, it can be seen that the proposed LDO can better track the actual disturbances than the conventional LDO with different conditions. Under the current transient and steady state tests, it can be seen that the proposed DPCC with LDO has the best current performance under multiple parameters mismatch compared with other DPCC. Therefore, the proposed DPCC with LDO can be promisingly applied in practical industrial applications to pursue high performance.

In terms of the future difficulties and challenges, although there is no need to obtain the actual inductance parameter and inverter disturbance by a start-up or offline commissioning procedure in the proposed DPCC with LDO, the accuracy of the inductance and inverter disturbance identification under low current and high speed conditions is not relatively high, and hence high accurate identification techniques should be developed. In addition, since the resistance parameter mismatch disturbance caused by the sudden q-axis reference current still negatively affect the DPCC with LDO, new disturbance evaluation approaches should be further studied in DPCC.

REFERENCES

[1] C. Liu, K. T. Chau, C. H. T. Lee, and Z. Song, "A critical review of advanced electric machines and control strategies for electric vehicles," *Proceedings of the IEEE*, pp. 1–25, 2020.
[2] V. Yaramasu and B. Wu, *Model predictive control of wind energy conversion systems*. John Wiley & Sons, 2016.
[3] Y. Wang, X. Wang, W. Xie, F. Wang, M. Dou, R. M. Kennel, R. D. Lorenz, and D. Gerling, "Deadbeat model-predictive torque control with discrete space-vector modulation for pmsm drives," *IEEE Transactions on Industrial Electronics*, vol. 64, no. 5, pp. 3537–3547, 2017.
[4] X. Yuan, C. Zhang, and S. Zhang, "A novel deadbeat predictive current control scheme for oew-pmsm drives," *IEEE Transactions on Power Electronics*, vol. 34, no. 12, pp. 11 990–12 000, 2019.
[5] Kiam Heong Ang, G. Chong, and Yun Li, "Pid control system analysis, design, and technology," *IEEE Transactions on Control Systems Technology*, vol. 13, no. 4, pp. 559–576, 2005.
[6] X. Zhang, L. Zhang, and Y. Zhang, "Model predictive current control for pmsm drives with parameter robustness improvement," *IEEE Transactions on Power Electronics*, vol. 34, no. 2, pp. 1645–1657, 2019.
[7] X. Yuan, S. Zhang, and C. Zhang, "Improved model predictive current control for spmsm drives with parameter mismatch," *IEEE Transactions on Industrial Electronics*, vol. 67, no. 2, pp. 852–862, 2020.
[8] X. Yuan, J. Chen, Y. Zuo, and C. H. T. Lee, "Deadbeat predictive current control considering inverter nonlinearity for permanent magnet synchronous machine drives," in *2021 IEEE Energy Conversion Congress and Exposition (ECCE)*, 2021, pp. 4955–4960.
[9] S. A. Odhano, R. Bojoi, Ş. G. Roşu, and A. Tenconi, "Identification of the magnetic model of permanent-magnet synchronous machines using dc-biased low-frequency ac signal injection," *IEEE Transactions on Industry Applications*, vol. 51, no. 4, pp. 3208–3215, 2015.
[10] Q. Wang, G. Wang, N. Zhao, G. Zhang, Q. Cui, and D. Xu, "An impedance model-based multiparameter identification method of pmsm for both offline and online conditions," *IEEE Transactions on Power Electronics*, vol. 36, no. 1, pp. 727–738, 2021.
[11] Y. Yao, Y. Huang, F. Peng, J. Dong, and H. Zhang, "An improved deadbeat predictive current control with online parameter identification for surface-mounted pmsms," *IEEE Transactions on Industrial Electronics*, vol. 67, no. 12, pp. 10 145–10 155, 2019.
[12] Z. Liu, H. Wei, X. Li, K. Liu, and Q. Zhong, "Global identification of electrical and mechanical parameters in pmsm drive based on dynamic self-learning pso," *IEEE Transactions on Power Electronics*, vol. 33, no. 12, pp. 10 858–10 871, 2018.
[13] C. Paleologu, J. Benesty, and S. Ciochina, "A robust variable forgetting factor recursive least-squares algorithm for system identification," *IEEE Signal Processing Letters*, vol. 15, pp. 597–600, 2008.
[14] L. Salvatore and S. Stasi, "Application of ekf to parameter and state estimation of pmsm drive," *Electric Power Applications, IEE Proceedings B*, vol. 139, pp. 155 – 164, 06 1992.
[15] Y. Zhang, Z. Yin, X. Sun, and Y. Zhong, "On-line identification methods of parameters for permanent magnet synchronous motors based on cascade mras," in *2015 9th International Conference on Power Electronics and ECCE Asia (ICPE-ECCE Asia)*, 2015, pp. 345–350.
[16] G. Pellegrino, R. I. Bojoi, P. Guglielmi, and F. Cupertino, "Accurate inverter error compensation and related self-commissioning scheme in sensorless induction motor drives," *IEEE Transactions on Industry Applications*, vol. 46, no. 5, pp. 1970–1978, 2010.
[17] Jong-Woo Choi and Seung-Ki Sul, "Inverter output voltage synthesis using novel dead time compensation," *IEEE Transactions on Power Electronics*, vol. 11, no. 2, pp. 221–227, 1996.
[18] D. Liang, J. Li, R. Qu, and W. Kong, "Adaptive second-order sliding-mode observer for pmsm sensorless control considering vsi nonlinearity," *IEEE Transactions on Power Electronics*, vol. 33, no. 10, pp. 8994–9004, 2017.
[19] X. Yuan, S. Zhang, and C. Zhang, "Enhanced robust deadbeat predictive current control for pmsm drives," *IEEE Access*, vol. 7, pp. 148 218–148 230, 2019.
[20] X. Yuan, S. Zhang, and C. Zhang, "Nonparametric predictive current control for pmsm," *IEEE Transactions on Power Electronics*, vol. 35, no. 9, pp. 9332–9341, 2020.
[21] J. Han, "From pid to active disturbance rejection control," *IEEE Transactions on Industrial Electronics*, vol. 56, no. 3, pp. 900–906, 2009.
[22] D. Luenberger, "An introduction to observers," *IEEE Transactions on Automatic Control*, vol. 16, no. 6, pp. 596–602, 1971.
[23] E. Sariyildiz, R. Oboe, and K. Ohnishi, "Disturbance observer-based robust control and its applications: 35th anniversary overview," *IEEE Transactions on Industrial Electronics*, vol. 67, no. 3, pp. 2042–2053, 2020.
[24] X. Zhang, L. Sun, K. Zhao, and L. Sun, "Nonlinear speed control for pmsm system using sliding-mode control and disturbance compensation techniques," *IEEE Transactions on Power Electronics*, vol. 28, no. 3, pp. 1358–1365, 2013.
[25] Q. Hou, S. Ding, and X. Yu, "Composite super-twisting sliding mode control design for pmsm speed regulation problem based on a novel disturbance observer," *IEEE Transactions on Energy Conversion*, vol. 36, no. 4, pp. 2591–2599, 2021.
[26] Y. Du, W. Cao, J. She, M. Fang, and Z. Lu, "An improved equivalent-input-disturbance approach for disturbance-rejection using high-gain observer*," in *2018 37th Chinese Control Conference (CCC)*, 2018, pp. 2643–2647.
[27] K.-S. Kim, K.-H. Rew, and S. Kim, "Disturbance observer for estimating higher order disturbances in time series expansion," *IEEE Transactions on automatic control*, vol. 55, no. 8, pp. 1905–1911, 2010.
[28] X. Zhang, B. Hou, and Y. Mei, "Deadbeat predictive current control of permanent-magnet synchronous motors with stator current and disturbance observer," *IEEE Transactions on Power Electronics*, vol. 32, no. 5, pp. 3818–3834, 2017.
[29] Hyun-Soo Kim, Hyung-Tae Moon, and Myung-Joong Youn, "On-line dead-time compensation method using disturbance observer," *IEEE Transactions on Power Electronics*, vol. 18, no. 6, pp. 1336–1345, 2003.
[30] Y. Zhang, J. Jin, and L. Huang, "Model-free predictive current control of pmsm drives based on extended state observer using ultralocal model," *IEEE Transactions on Industrial Electronics*, vol. 68, no. 2, pp. 993–1003, 2021.

Response to Review of Manuscript ID JESTPE-2021-12-1420 "An Enhanced Deadbeat Predictive Current Control of SPMSM with Linear Disturbance Observer"

Dear Editor,

The Authors would like to thank the Editor in Chief for considering the manuscript and following his/her suggestion, the paper has been revised according to the Reviewers' comments. The Authors have worked to update the paper and all the questions raised by the Reviewers have been addressed leading to a significant improvement of the work quality. Finally, the Authors would like to thank the Reviewers, whose feedbacks have been constructive and insightful. Please find hereafter our replies and main changes to the paper. Changes in our manuscript have been marked in blue color.

Main changes in the revised Manuscript:

In accordance with the editors' and reviewers' comments, the following major modifications have been made:

1. In order to further enhance the paper quality, the new test results raised by reviewers have been carried out, i.e., Fig.11 and Figs.13-16. In addition, the computation time of the three methods has been shown.

2. The flow chart of the proposed DPCC with LDO has been shown to simplify the idea for the readers.

3. We have proofread the manuscript thoroughly to avoid grammar mistakes and typos.

Sincerely,
The Authors.

2. Response to Associate Editor:

Q1:There are pertinent questions raised by the reviewers about the novel contribution of the manuscript and the advantages of the methodology proposed. These have to be addressed by the authors adequately. So, a major revision is to be done by the authors as per the reviewers' comments.

A1:The Authors would like to thank Associate Editor for reviewing our paper. In our methodology proposed, the 3rd order LDO is established and a new inductance and nonlinearity inverter observer is proposed, which can work so well with DPCC. In order to evaluate the performance of the proposed method, three different DPCC have been compared. The issues raised by the three reviewers have been fully solved. In our revised paper, new test results have been added in the revision to validate the proposed method has the best current performance under different conditions. In addition, we have proofread the manuscript thoroughly to avoid grammar mistakes and typos. Finally, the flow chart of the proposed DPCC with LDO has been shown to show the novel contribution of the manuscript and the advantages of the methodology proposed.

3. Response to Reviewer 1:

Q1: Generally, this paper is well-written and provides an effective high order LDO to achieve better parameter robustness in DPCC. However, several minor problems in the manuscript are needed to be addressed. In the Section-III-C. Why LDO cannot evaluate the disturbance under high speed condition? Please clarify in detail.

A1:Thank you for recognizing our work. Because of the limitation of the system sampling frequency, the value of the bandwidth of LDO cannot be increased so much. This is a reason that LDO should be combined with the proposed inductance and inverter disturbance observer.

Considering current measurement noises $\sigma_{\mathbf{dq}}$, the estimated disturbance equation $\mathbf{F(s)}$ of the proposed DPCC with LDO in s domain is presented as:

$$\frac{\widehat{\mathbf{D_{dq2}}(\mathbf{s})}}{T_s s\sigma_{\mathbf{dq}}(\mathbf{s})+T_s[\frac{\mathbf{U^{ref}_{dq}(s)}-\mathbf{U'_{dq}(s)}}{L_s}-\frac{\mathbf{U^{ref}_{dq}(s)}-\widehat{\mathbf{U'_{dq}(s)}}}{\widehat{L}}]+\mathbf{D_{dq2}(s)}}=\mathbf{F(s)}$$
$$\mathbf{F(s)}=\frac{-\frac{\gamma_3}{T_s^2}}{s^3+\gamma_1 s^2-\frac{\gamma_2}{T_s}s-\frac{\gamma_3}{T_s^2}} \tag{1}$$

The proposed LDO coefficients γ_1, γ_2, and γ_3 can be designed as:

$$\begin{cases}\gamma_1=3w_n\\ \gamma_2=-3T_s w_n^2\\ \gamma_3=-T_s^2 w_n^3\end{cases} \tag{2}$$

It can be seen that the estimated disturbance transfer function $\mathbf{F(s)}$ can be expressed as $\mathbf{F(s)}=\frac{w_n^3}{(s+w_n)^3}$. If the frequency of the disturbance is larger (the frequency of the inverter nonlinearity under high speed condition is larger), the LDO cannot evaluate.

Q2:In the Section-III-C: Because the resistance, inductance and rotor flux linkage parameters cannot vary fast due to SPMSM property. If the parameters vary fast, How can LDO work to eliminate these disturbances?

A2:Thanks for your comments.You are right. For the resistance, inductance and rotor flux linkage parameters, it can not be changed fast in SPMSM. If the parameters vary fast, the bandwidth of LDO should be tuned to higher value to eliminate these disturbances. This is inherent limitation of LDO in digital controller.

Q3:In Eq. (26), Would you please explain the derivation of Z(s)?

A3:Thanks for your comments. $Z(s)$ can be simply chosen as the first order inertia. With the increase of f_{b2}, the observer speed is enhanced, but the high frequency noise will be amplified. $Z(s)$ can be shown as $Z(s) = \frac{w_n}{s+w_n}$.

If the following term is satisfied as: $Z(s) = \frac{w_n}{s+w_n}$, the closed-loop of the inductance and inverter disturbance observer can be simplified as first order low-pass filter system, which can accurately estimate the inductance parameter and distorted voltage caused by inverter nonlinearity without overshoot.

Q4:In this paper, you are employing the first-order forward Euler discretization, why don?t you try other discretization methods, e.g., Tustin?

A4:Thanks for your comments. Other discretization methods, i.e., Tustin and back Euler discretization can also be employed herein in our proposed DPCC with LDO. The first-order forward Euler discretization is the simplest way to discrete the continuous system to discrete system.

Q5:In the proposed DPCC with LDO performance evaluation part of Section-IV, would you further explain the high frequency disturbance performance is improved in the proposed method?

A5:Thanks for your comments. In terms of the inverter disturbance, without employing the start-up and offline inverter nonlinearity commissioning methods, the proposed LDO is able to acquire $\mathbf{U}_{\mathbf{dq}}^{'}$. $\mathbf{D_{dq2}(s)}$ does not include $\mathbf{U}_{\mathbf{dq}}^{'}$, which means that the proposed LDO cannot be affected by the inverter disturbance under high speed condition. In addition, it can be seen that the dq-axis coupling inductance voltages $\mathbf{G}$ are not considered in total disturbances and the sudden q-axis reference current cannot affect the proposed LDO on d-axis compared with $\mathbf{D_{dq1}}$. In this case, the high frequency disturbance caused by the sudden q-axis reference current effect on the proposed DPCC with LDO is reduced. This is a main reason that the high frequency disturbance performance is improved in the proposed method.

Q6:There exist few grammar mistakes and typos, the authors are required to check this paper thoroughly.

A6:Thanks for your comments in our paper. According to your suggestion, we have proofread the manuscript thoroughly to avoid this kind of mistake.

4. Response to Reviewer 2:

Q1:How to design the LDO coefficients in the proposed method when the model parameters are mismatched.

A1:Thanks for your comments in our paper. When the model parameters are mismatched, the LDO coefficients should be set suitably to estimate the lumped disturbances. The detailed for the LDO coefficients design is presented as follows:

Without considering the measurement noise and inverter non-linearity, based on Eqs. (19)-(20) of the revised paper, the estimated disturbance equation of the proposed DPCC with LDO in s domain can be presented as:

$$\frac{\widehat{\mathbf{D_{dq2}(s)}}}{\mathbf{D_{dq2}(s)}} = \frac{-\frac{\gamma_3}{T_s^2}}{s^3 + \gamma_1 s^2 - \frac{\gamma_2}{T_s}s - \frac{\gamma_3}{T_s^2}} \tag{3}$$

In order to set the estimated disturbance transfer function as $\frac{w_n^3}{(s+w_n)^3}$, the proposed LDO coefficients γ_1, γ_2, and γ_3 can be designed as:

$$\begin{cases} \gamma_1 = 3w_n \\ \gamma_2 = -3T_s w_n^2 \\ \gamma_3 = -T_s^2 w_n^3 \end{cases} \tag{4}$$

From the transfer function $\frac{w_n^3}{(s+w_n)^3}$, it can be known that the proposed LDO is stable and steady state error is zero. The LDO convergent speed is increased as the value of w_n enhancing. The $\frac{w_n^3}{(s+w_n)^3}$ transfer function looks like the first order low-pass filter $\frac{w_n}{s+w_n}$, where w_n is the LDO cut-off frequency.

Q2:What about the stability of the proposed LDO when the model parameters are mismatched.

A2:Thanks for your comments herein. Since the estimated disturbance transfer function is $\frac{w_n^3}{(s+w_n)^3}$, the proposed LDO stability can be controlled by the value of w_n. w_n is related to LDO bandwidth and the bandwidth should be much lower than sampling frequency to make a stable system. In this case, as long as the value of w_n is not quite high e.g., $w_n < 2\pi 500$rad/s, the proposed LDO will be stable.

Q3:What about the computational burden of the proposed method.

A3:Thanks for your suggestions. The computational burden of the proposed method has been carried out in the TABLE IV of the revised paper. The computation time of the proposed DPCC is only about 3.4 μs more than that in DPCC with LDO, but the transient and steady state current performance of the test results is much improved under different parameter mismatch conditions.

Q4:What about the high speed control performance.

A4:Thanks for your suggestions in our paper. In our paper, the new test results under the rated speed condition have been carried out in Fig.15 of the revised paper. it can be shown that there is a large dc offset in dq-axis current for DPCC while the DPCC with LDO and proposed DPCC with LDO can suppress the disturbances caused by parameter mismatch. Furthermore, it can be seen that the large fluctuation occurs in the DPCC with LDO under this multiple parameters mismatch and the proposed DPCC can own the best current performance under the multiple parameters mismatch.

Because that this paper only focuses on DPCC with LDO under the normal speed condition (the zero speed to rated speed condition), flux-weakening condition is not a focus in our paper.

Q5How to analyze the dynamic control performance of the proposed method to verify the validity of the results shown in Fig.12.

A5:Thank you for comments in our paper. In order to shown the superiority of the proposed method, Fig.12 has been redone and shown in Fig.14 of the revised paper. In Fig.14, it can be seen that when the value of the initial inductance is smaller than the actual inductance, the dynamic response becomes relatively slow and the slight q-axis current overshoot occurs in Fig.14(b), while the best q-axis dynamic response occurs in (c). It can be seen that the dq-axis offset current occurs in Fig.14(a). Due to adding inductance and inverter disturbance observer, the current fluctuation of the proposed DPCC is smallest among the three methods. The q-axis current settling time (within 5 $\%$ of its final value) of the three methods is 45ms, 23ms, and 12ms, respectively. The d-axis current settling time of the three methods is 50ms, 6ms, and 2ms, respectively. When the nominal inductance is about two times larger than the actual inductance, the system stability of the DPCC and DPCC with LDO will be deteriorated and the larger current fluctuation will happen, which is similar as shown in Fig.15 of the revised paper.

4. Response to Reviewer 3:

Q1:Please, proofread the manuscript for general typos corrections such as. The paragraph in lines 50-59, page 4, left column, contain typo errors.

A1:Thanks for your comments in our paper. According to your suggestion, we have proofread the manuscript to avoid this kind of mistake.

Q2:Please, improve the literature review to consider all existing disturbance observer schemes.

A2:Thanks for your suggestions herein. The three different types of disturbance observers have been added in the introduction part, i.e., high-gain disturbance observer, high order disturbance observer and super-twisting sliding mode disturbance observer. Also, the corresponding references have been added in the revised paper, which as shown as follows:

[25] Q. Hou, S. Ding, and X. Yu, "Composite super-twisting sliding mode control design for pmsm speed regulation problem based on a novel disturbance observer," *IEEE Transactions on Energy Conversion*, vol. 36, no. 4, pp. 2591–2599, 2021.

[26] Y. Du, W. Cao, J. She, M. Fang, and Z. Lu, "An improved equivalent-input-disturbance approach for disturbance-rejection using high-gain observer*," in *2018 37th Chinese Control Conference (CCC)*, 2018, pp. 2643–2647.

[27] K.-S. Kim, K.-H. Rew, and S. Kim, "Disturbance observer for estimating higher order disturbances in time series expansion," *IEEE Transactions on automatic control*, vol. 55, no. 8, pp. 1905–1911, 2010.

Q3:The proposed DPCC-LDO uses two estimation steps, which increases the computational burden. Please, compare the computational burden of the proposed and conventional schemes.

A3:Thanks for your comments. The computational burden of the proposed and conventional schemes has been shown in Table.IV of the revised paper. The computation time of the proposed DPCC is only about 3.4 μs more than that in DPCC with LDO, but the transient and steady state current performance of the test results is much improved under different parameter mismatch conditions.

Q4:What is the selected value of the tunable coefficient?

A4:Thanks for your comments in our paper. δ_2 is related to the inverter parameters and the range of δ_2 is $(0, \frac{\pi}{6})$ and the smaller the value is chosen, the slower the estimated speed is. The value of δ_2 is $\frac{\pi}{12}$ in the experimental results.

Q5It is well-known that the significant negative effects of the parameters'mismatches and disturbances come from the inductance and inverter non-linearity disturbances. The effects of the resistance and rotor flux mismatches are not significant, as shown by Fig. 13 (b), (d), and (f). Hence, what is the importance of using the LDO, if the inductance and inverter non-linearity disturbances are observed separately?

A5:Thanks for your comments in our paper. LDO can be utilized to estimate the slowly varying disturbances, i.e., the disturbances caused by the resistance and flux linkage mismatch, whereas the the inductance and inverter non-linearity disturbance observer can only estimate the disturbances caused by inductance mismatch and inverter non-linearity. In other words, the LDO and inductance and inverter non-linearity disturbance observer will handle slowly and quickly varying disturbances, respectively. Therefore, it is the importance of using LDO in the DPCC scheme.

In order to validate it, Fig.16 has been carried out in the revised paper, and it can be seen that there exists q-axis dc-offset current variation under the resistance and flux linkage parameters mismatch. Therefore, the LDO should be combined with the inductance and inverter non-linearity disturbance observer.

Q6Please, include a result section to compare the DPCC using only proposed inductance and inverter disturbances observer with the proposed DPCC-LDO.

A6:Thanks for your suggestions in our paper. The new test has been carried out in Fig.16 of the revised paper, which is shown as here.

From the result, it can be seen that there exists a q-axis dc offset current (over the value of reference current (4A)) in the DPCC with inductance and inverter disturbance observer, which mean that it cannot suppress the disturbances caused by rotor flux linkage and resistance compared with the proposed DPCC.

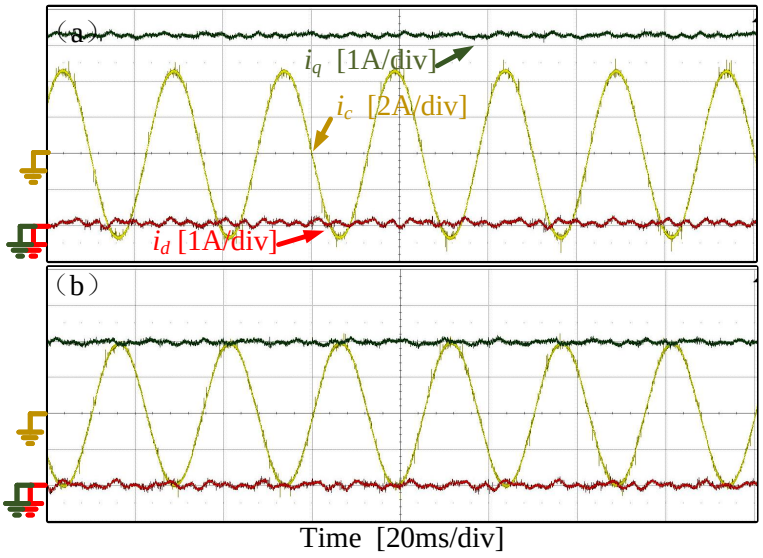

Fig. 1: dq-axis current performance under 600rpm speed condition. (a) Conventional DPCC with inductance and inverter disturbance observer under $\psi_{m0} = 1.5\psi_m, R_{s0} = 2R_s$; (b) Proposed DPCC under $\psi_{m0} = 1.5\psi_m, R_{s0} = 2R_s$.

Q7To verify the effectiveness of the proposed inductance and inverter disturbance observer, the steady state performance of the proposed DPCC-LDO with and without inductance and inverter disturbance observer should be quantitively compared under different parameters mismatches conditions.

A7:Thanks for your suggestions in our paper. The steady state performance of the proposed DPCC-LDO with and without inductance and inverter disturbance observer has been carried out in Fig.11 of the revised paper, which is also shown herein.

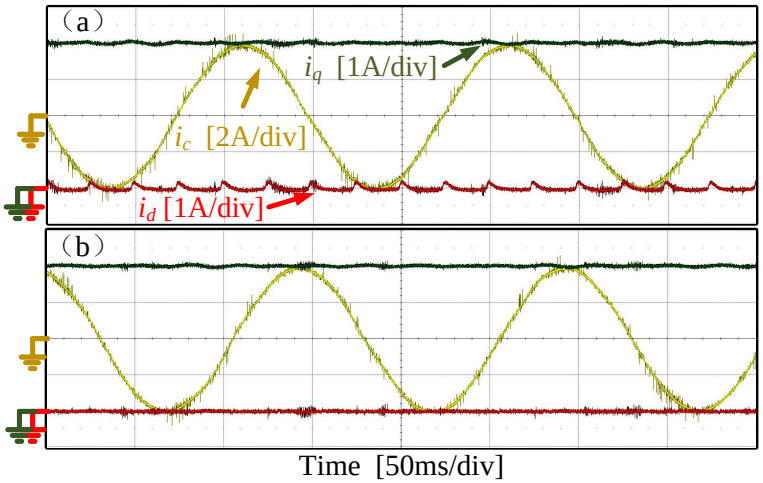

Fig. 2: The current performance under 100rpm speed condition. (a) DPCC with proposed LDO without using inductance and inverter disturbance observer; (b) DPCC with proposed LDO using inductance and inverter disturbance observer.

From the test results, it can be seen that d-axis current harmonic is reduced, which can show

that the disturbance caused by inverter nonlinearity is suppressed compared with DPCC with LDO without using inductance and inverter disturbance.

Q8The performance of the studied schemes should be quantitively compared under different operating conditions using parameters such as current ripples, torque ripples and settling times, etc.

A8:Thanks for your suggestions in our paper. In Fig.14 of the revised paper, the settling time (within 5 % of its final value) of the three methods is computed, which is 45ms, 23ms, and 12ms, respectively. In addition, in Fig.15 of the revised paper, the total harmonic distortion of the three methods are 4.49%, 7.71% and 2.86%. Based on the above quantitative test results, the proposed DPCC can own the best current performance under different operating conditions.

Q9Figs. 10-11 should include the performance of the proposed DPCC-LDO under different inductance mismatches.

A9:Thanks for your comments in our paper. There is no need for the nominal inductance parameter involved in the proposed DPCC-LDO where the inductance and inverter nonlinearity observer will help to estimate the actual inductance. In other words, the initial inductance parameter is not involved in the proposed DPCC-LDO and the performance of the proposed DPCC-LDO under different inductance mismatches is the same.

Q10 The results of Fig. 11 should be implemented at a high speed such as 1000 r/min instead of 200 r/min.

A10:Thanks for your suggestions in our paper. The new test result about the disturbance performance under 1000 r/min has been carried out in the revised paper, which is shown in Fig.13 of the revised paper.

Q11 What are the advantages of the proposed LDO scheme over the improved current variation update mechanism [R1]? References [R1] X. Yuan, S. Zhang, and C. Zhang, ”Improved Model Predictive Current Control for SPMSM Drives with Parameter Mismatch,” IEEE Trans. Ind. Electron., vol. 67, no. 2, pp. 852-862, Feb. 2020.

A11:Thanks for your comments in our paper. In [R1], the method is based on the current variation update mechanism to estimate the inductance of SPMSM and the method can only be utilized in MPCC (Model predictive current control) and cannot be employed in DPCC (deadbeat predictive current control). The reason behind this is that MPCC has only use one

voltage vector within one control period and the current variation applied voltage vector is larger than that in DPCC (using SVPWM, there exists two different voltage vectors and two zero voltage vectors). Thus, the induction estimation can be accuarte in MPCC. However, this method cannot be employed in DPCC because of almost the same current variation at steady state.

In addition, in terms of DPCC with LDO, the merit of the method (proposed LDO with inductance and inverter nonlinearity observer) is universal for different current controller and can be extended to MPCC.

Q12 Adding flow chart to summarize the proposed DPCC-LDO scheme can simplify the idea for the readers.

A12:Thanks for your precious suggestions in our paper. The flow chart of the proposed DPCC-LDO scheme has been added in the revised paper, as also shown herein.

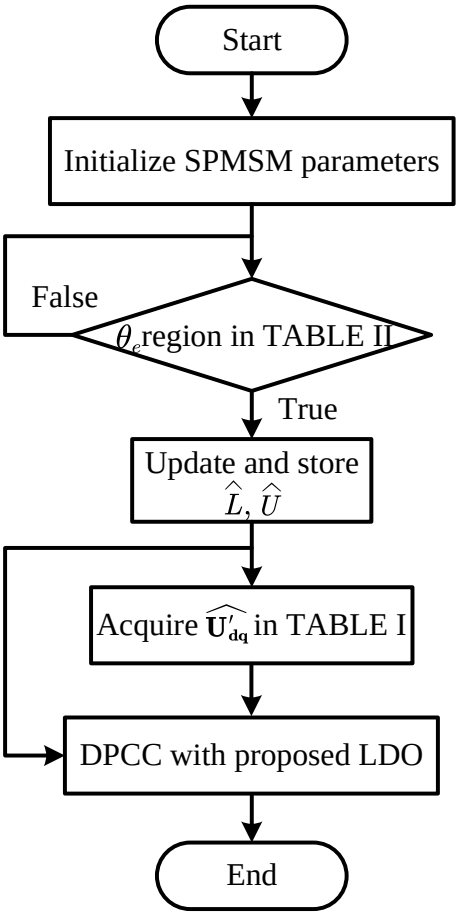

Fig. 3: Flow chart of the proposed DPCC with LDO.

Q13 There is not a clear difference between the studied schemes under the resistance and rotor-flux mismatch, as shown by Fig. 13 (b), (d), and (f).

A13:Thanks for your comments in our paper. Since the figure is quite small and the test results have been redone, which as shown in Fig.15 of the revised paper.

It can be seen that there is a large dc offset in dq-axis current for DPCC while the DPCC with LDO and proposed DPCC with LDO can suppress the disturbances caused by parameter mismatch. Furthermore, it can be seen that the large fluctuation occurs in the DPCC with LDO under this multiple parameters mismatch and the proposed DPCC can own the best current performance under the multiple parameters mismatch.

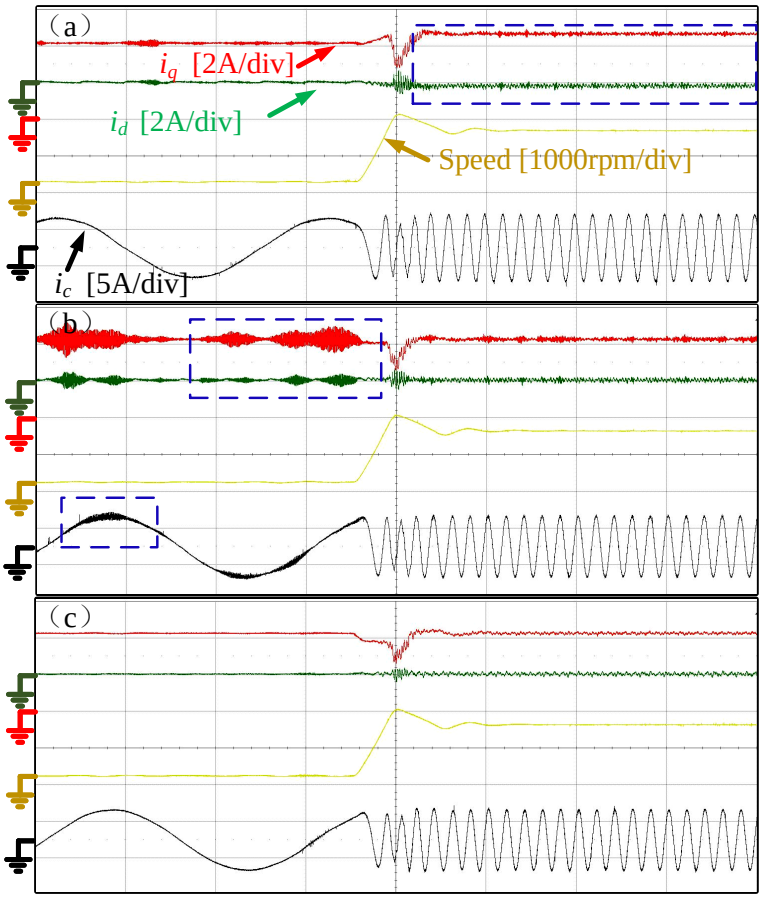

Fig. 4: Three DPCC methods performance comparison. (a), (b) and (c) Conventional DPCC, conventional DPCC with LDO and proposed DPCC under $L_{s0} = 1.85L_s, \psi_{m0} = 1.5\psi_m, R_{s0} = 0.5R_s$ and 100rpm to 1500rpm speed condition.